SeaSAR 2023: Wave retrieval session

Authors : Pleskachevsky, Andrey; Tings, Björn; Jacobsen, Sven; Kleinherenbrink, Marcel; Ehlers, Frithjof; Gibert, Ferran; Fernandez, Sergi; Nouguier, Frederic; Chapron, Bertrand; Lopez-Dekker, Paco; Rikka, Sander; Nõmm, Sven; Alari, Victor; Björkqvist, Jan-Victor; Simon, Martin; Khan, Salman Saeed; Ocampo-Torres, Francisco; Osuna, Pedro; García-Nava, Héctor; Díaz Méndez, Guillermo; Esquivel-Trava, Bernardo; Villarreal-Olavarrieta, Carlos; Mora-Escalante, Rodney; Hasimoto-Beltrán, Rogelio; Benchaabane, Amine; Husson, Romain; Mouche, Alexis; Johnsen, Harald; Aouf, Lotfi; Hauser, Danièle; Collard, Fabrice; Amir, Malik Muhammad Haris; Bogoni, Antonella; Pouplin, Clément; Yourovkaya, Maria; Guitton, Gilles.

Main conclusions

Wave spectra on a subscene-by-subscene basis are poorly constrained.

- Cut-off limits the directional sensitivity.
- Continuity should be exploited (Fireworks/models/statistical/group analysis).
- Wind-wave system should be better constrained (models/feature analysis).
- RAR can be improved (multi-sensor observations/multi-line-of-sight Harmony).
- Multi-scale neural-network approaches show potential.

Stress-equivalent wind, wave-Doppler, currents and long-ocean waves should be integrally estimated.

- All observations originate from the same surface.
- NRCS, Doppler, SAR spectra should be combined in one assimilation (neural networks).
- Neural networks for full spectra, not only integral parameters.
- Causal filtering in iterative approaches or external wind and waves models.

Air-sea-wave interactions

Air-wave interactions:

- Wind stress.
- Wave growth.
- Turbulence.

Wave-wave interactions:

- Wave-breaking and hydrodynamic modulation.
- Three and four wave interactions.
- Coupling.

Sea-wave interactions:

- Wave-breaking.
- Current generation.
- Refraction.

Fluxes:

- Heat exchanges.
- Gas exchanges (CO_2, etc.).
- Aerosols (salt, etc.).
- Momentum, ….

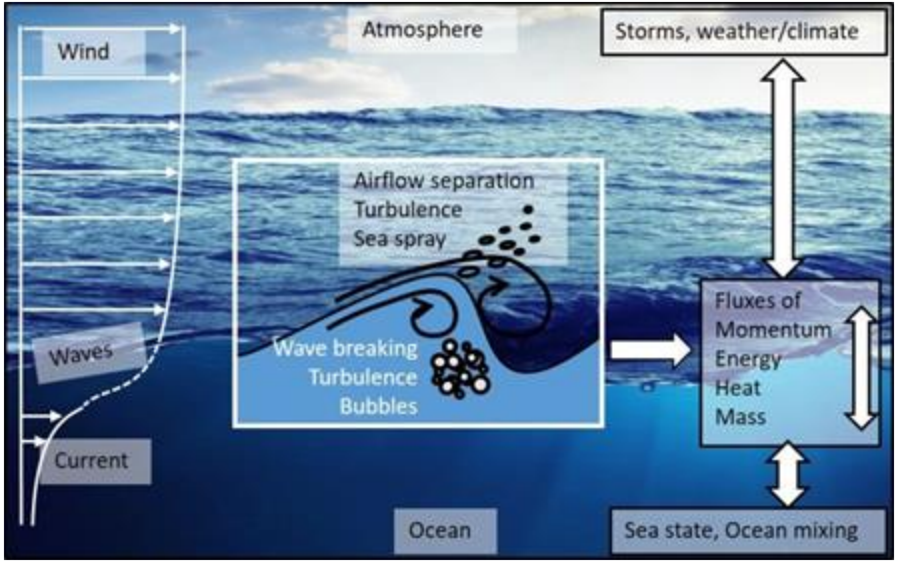

Marc Buckley, Helmholtz Centrum

Spaceborne instruments

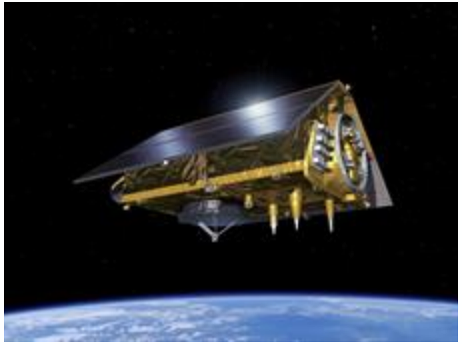

Satellite radar altimeters (Sentinel-6)*

Multispectral imagers (Sentinel-2)*

Synthetic aperture radars (Sentinel-1)*

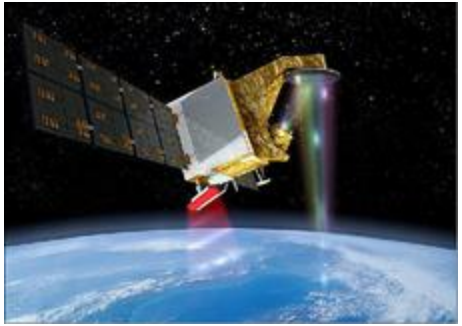

*Spectrometers (CFOSat**)*

*Satellite lidar altimeters (ICESat-2***)*

Courtesy of ESA, eoPortal** and NASA****

Observing geometry and scattering mechanisms

Incident angle

S6	CFO	S1 WM	S1 IW
0.3-0.7°	2-10°	23-36°	31-46°

*Sentinel-6** *CFOSat*** *Sentinel-1****

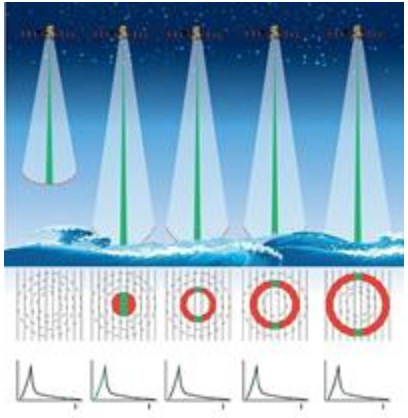

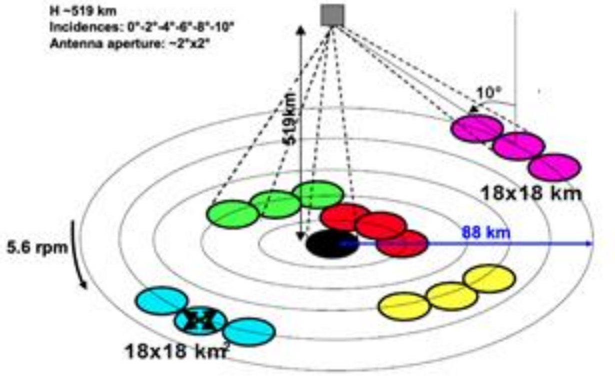

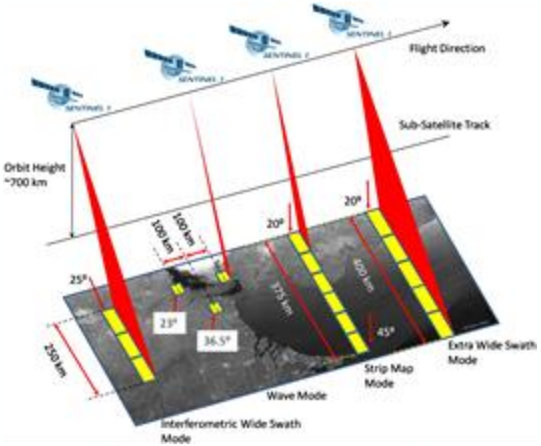

Specular scattering ⟷ Resonant scattering

⟵ Wave breaking ⟶

Courtesy of AVISO, Hauser et al. 2006** and ESA****

Imaging mechanisms

RAR

- Tilt modulation
  - near-nadir: weak/moderate, far-field: weak.
  - direction: range.
- Hydrodynamic modulation (not shown):
  - near-nadir: very weak, far-field: weak.
  - direction: omnidirectional.
- Range shifts and range bunching:
  - near-nadir: very strong, far-field: very weak.
  - direction: range.
  - near-nadir: (very) non-linear, decreases range resolution.

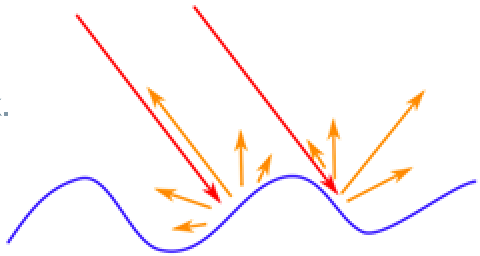

Tilt modulation

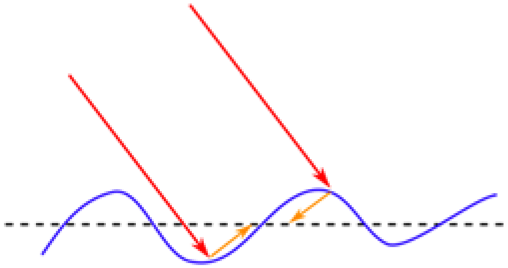

Range bunching

SAR

- Doppler shifts and velocity bunching:
  - near-nadir: strong, far-field: strong.
  - direction: azimuth.
  - near-nadir: non-linear, far-field: non-linear.
  - decreases azimuth resolution.

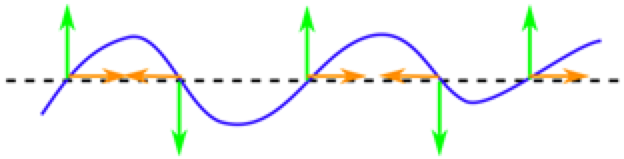

Velocity bunching

Closed-form mapping: misregistration in space, phase changes in Fourier domain

- Spectral mapping (Hasselmann & Hasselmann, 1991; Krogstad et al. 1992/1994).
- The misregistration is associated to both range and azimuth random shifts.
- Azimuth shifts are directly associated to detected scatter velocities: it can be polarization and wavelength dependent.
- Shifts scale with the R/V parameter.
- Under joint-Gaussian statistical assumption (and stationary conditions), a spectral closed form can be derived:

$$P(k_x,k_y) = \frac{1}{(2\pi)^2}\int\int G(x,y,k_x,k_y)e^{-i(k_x x+k_y y)}dxdy$$

$$P(k_x,k_y) = \frac{1}{(2\pi)^2}e^{-k_x^2\rho_{xx}(0,0)-k_y^2\rho_{yy}(0,0)-k_xk_y(\rho_{xy}(0,0)+\rho_{yx}(0,0))}\int\int e^{k_x^2\rho_{xx}+k_y^2\rho_{yy}+k_xk_y(\rho_{xy}+\rho_{yx})}Le^{-i(k_x x+k_y y)}dxdy,$$

$$\rho_{ab} = \frac{1}{(2\pi)^2}\int\int \frac{1}{2}T_a(k_x,k_y)T_b^*(k_x,k_y)S(k_x,k_y)+\frac{1}{2}(T_a(-k_x,-k_y)T_b^*(-k_x,-k_y))^*S(-k_x,-k_y)e^{i(k_x x+k_y y)}dk_xdk_y$$

Cross-spectral analysis

- Introduced by Engen & Johnsen (1995).

$$\rho_{ab} = \frac{1}{(2\pi)^2} \int\int \frac{1}{2} T_a(k_x,k_y) T_b^*(k_x,k_y) e^{-i\omega\Delta t} S(k_x,k_y) + \frac{1}{2} \left(T_a(-k_x,-k_y) T_b^*(-k_x,-k_y) e^{-i\omega\Delta t}\right)^* S(-k_x,-k_y) e^{i(k_x x + k_y y)} dk_x dk_y$$

- Speckle noise bias (Goldfinger, 1982) absent in cross-spectra.
- Determination of wave direction.

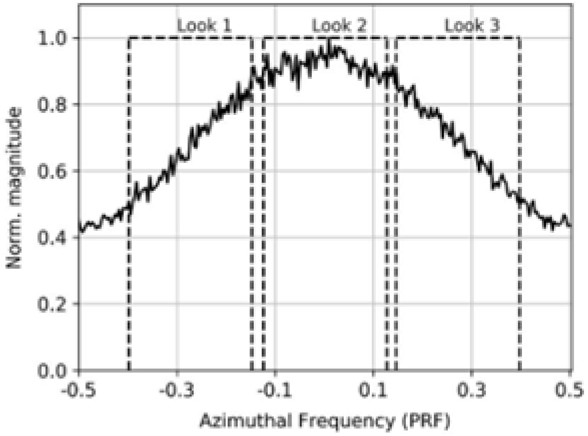

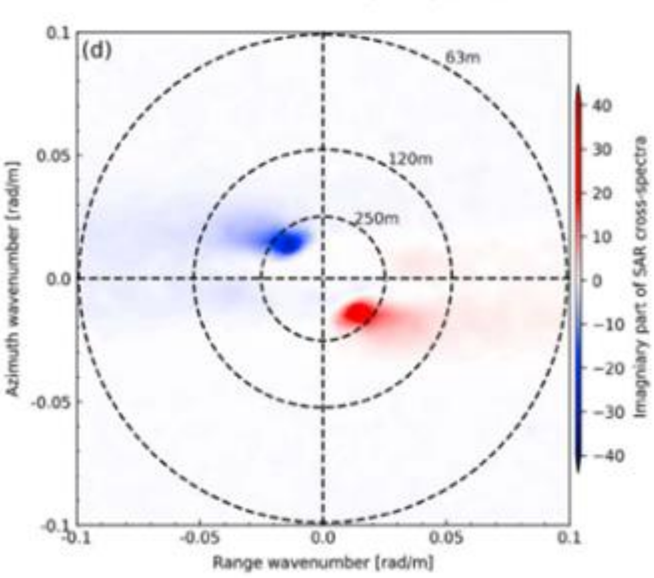

Figures from Li et al. (2019)

Cross-spectral phase and dispersion relation

- Mean dispersion relation for low wind speeds (red) and high (blue) . Data extracted from s1b wv ocn data (full lines) along range axis. The **dashed lines are simulated dispersion relation including effects of non-linear RAR modulation and non-stationarities.** The dotted line is the wave dispersion relation of linear SAR wave imaging along range axis.

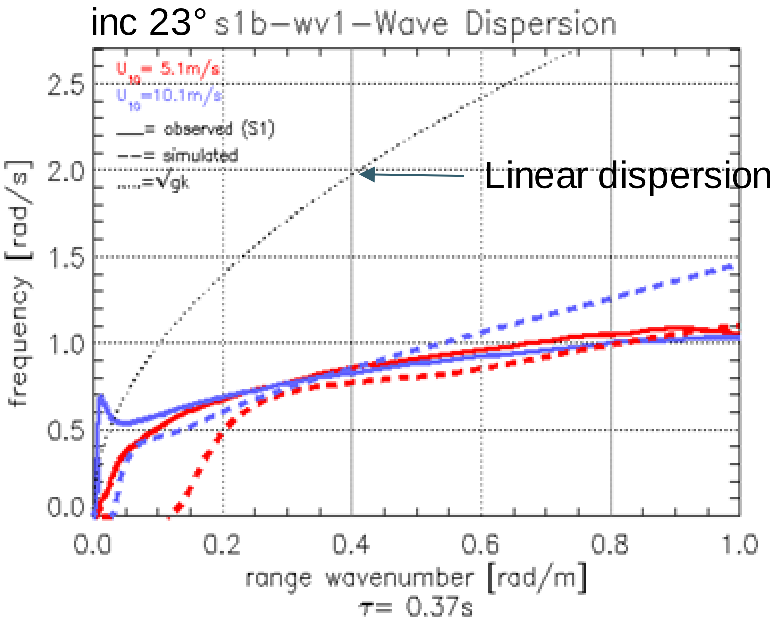

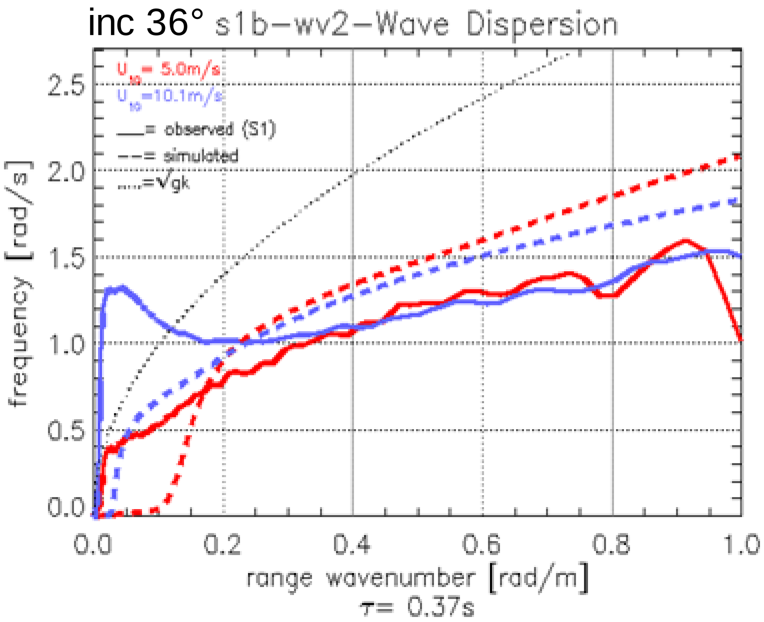

Cross-spectral phase and dispersion relation

- Sentinel-1 **TOPS mode** analysis of **burst overlap area**

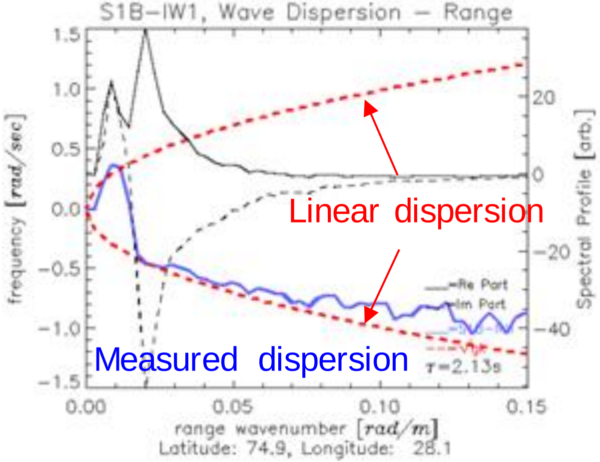

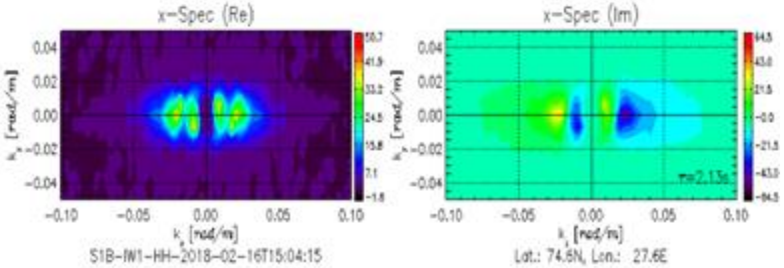

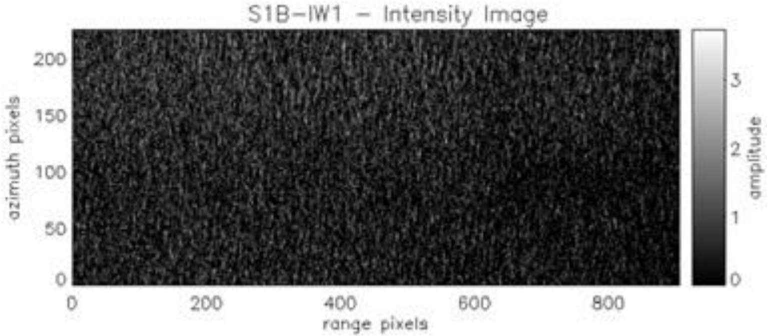

IMACS

- Integral in range direction of cross-spectrum (Li et al. 2019).
- Measurable time-evolution of detected scales between 15-20 m wavelength range.
- Important for wave-Doppler removal.

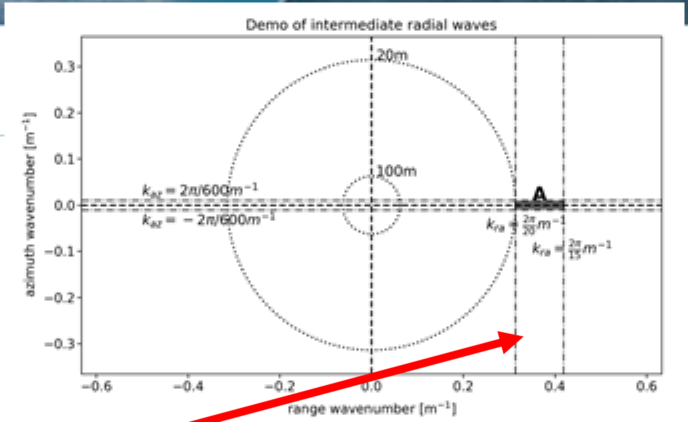

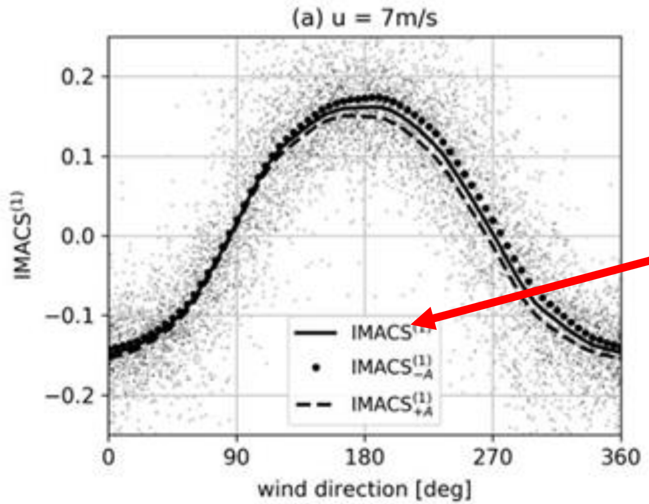

Figures from Li et al. (2019)

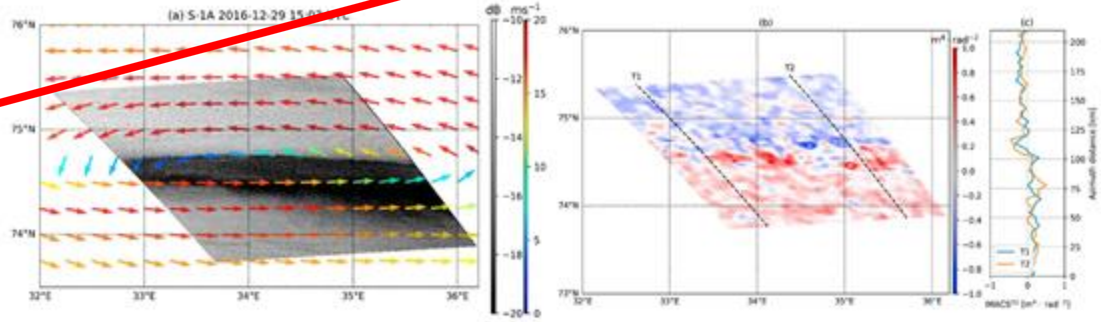

IMACS

- Systematic and massive computation of x-spectra @17.7 km from Sentinel-1 IW SLC products allowed for statistical analysis of IMACS to refine Li et al. (JGR 2019) analysis.
- About 180,000 x-spectra have been colocated with ECMWF and WW3 model outputs
- In the contrary of VV, the IMACS sensitivity to geophysical parameters is found negligible in VH on the dataset used for this study.
- A Strong dependence is found with respect to wind speed and direction.
- An Asymmetry is obtained between Upwind and Downwind absolute values. Upwind>downwind. Second order effect.
- The incidence angle dependence is also found to be a second order effect.

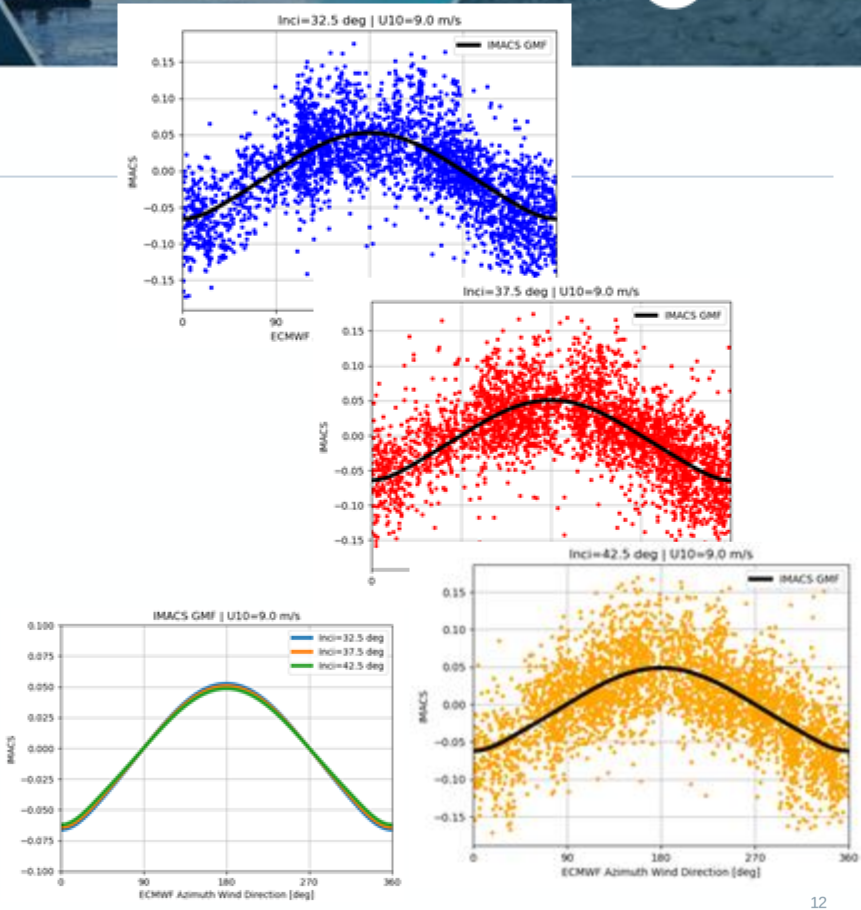

sarwave

Cut-off estimation

- Estimated by fitting a Gaussian to the ACF (Vachon et al. 1993; Kerbaol et al. 1998).
- Proportional to the velocity variance.
- Required to constrain the wind-wave spectrum, e.g. the wave-age parameter.
- Removal of the non-linear part in the Sentinel-1 OSW spectra (Sentinel-1 ATBD).

Figures from Stopa et al. (2019)

wave orbital velocity (m/s)

$$\lambda_c \propto \pi\sqrt{\rho_{yy}(0,0)} = \pi\frac{R}{V}\sqrt{\sigma_v^2}$$

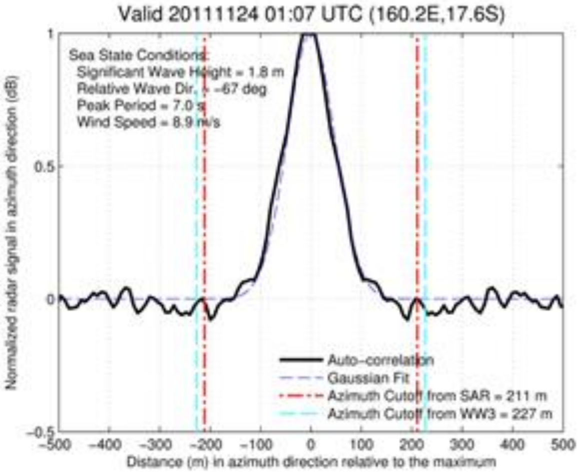

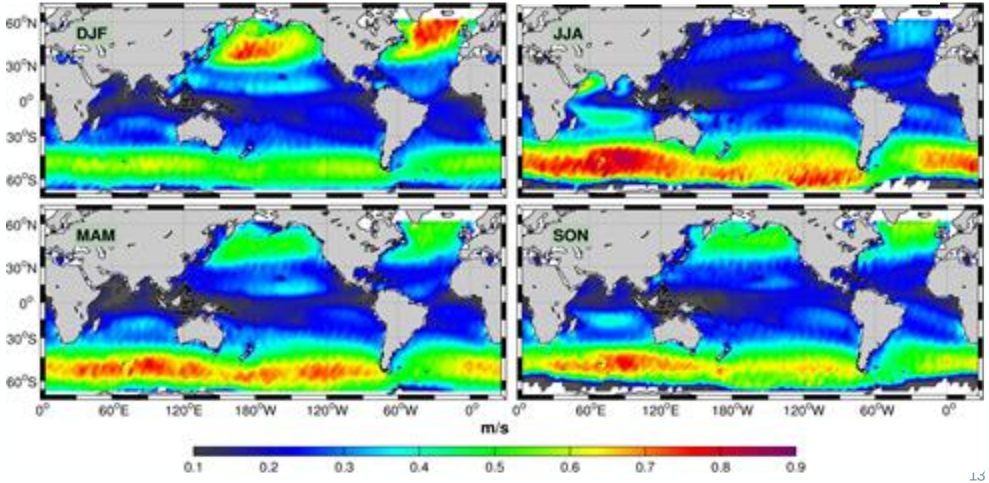

Cut-off fitting issues

- Limited surface roughness at low wind speeds.
- Overestimation because scene is not properly resolved.
- Underestimation with swell in the range direction.

- Resolved waves affect the cut-off estimation.
- Waves in the azimuth direction can introduce sinc-like behavior.
- Steep waves across track cause underestimation.
- Lower waves across track cause underestimation.

- Only empirical corrections (Stopa et al. 2015).
- Possible mitigation: to use the second derivative of the first lags of the autocorrelation function in azimuth.

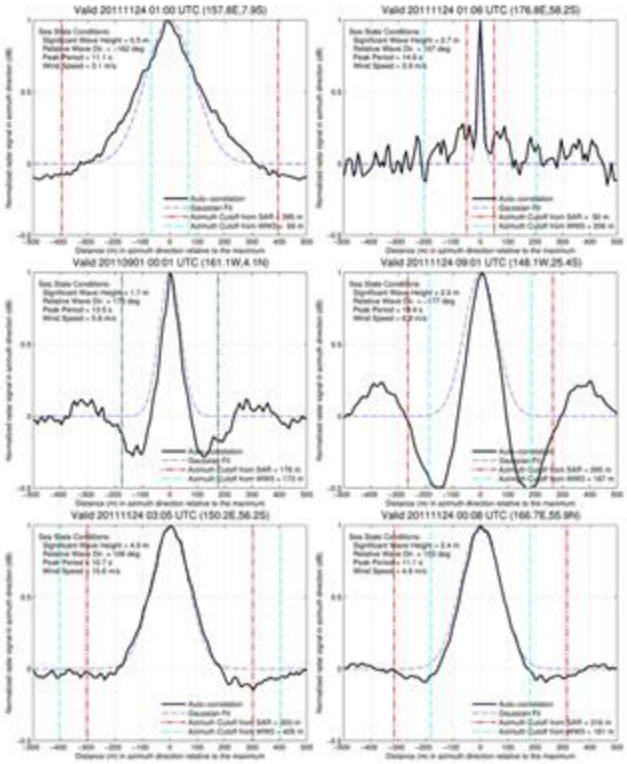

Figure from Stopa et al. (2019)

Spectral width

- Fall-off with increasing azimuth wavenumber (Lyzenga et al. 1986).

$$k_y \to \infty \qquad P(k) \to \frac{1}{\alpha k_y^4}$$

- Spectral domain 'cut-off' (Engen & Johnsen, 2002).
- Parameter is computed in the Sentinel-1 OSW products.
- Related to wind-wave VV and NRCS.
- Useful for calibration.

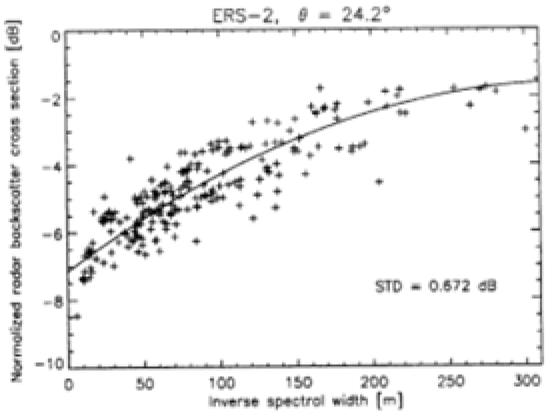

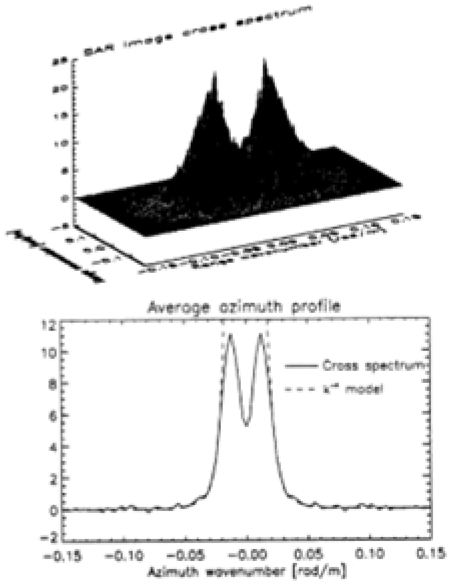

Figures from Engen & Johnsen (2000)

Retrieval algorithms

- Closed-form approaches:
  - Iterative Max-Planck.
  - Self 2-step approach (no a priori).

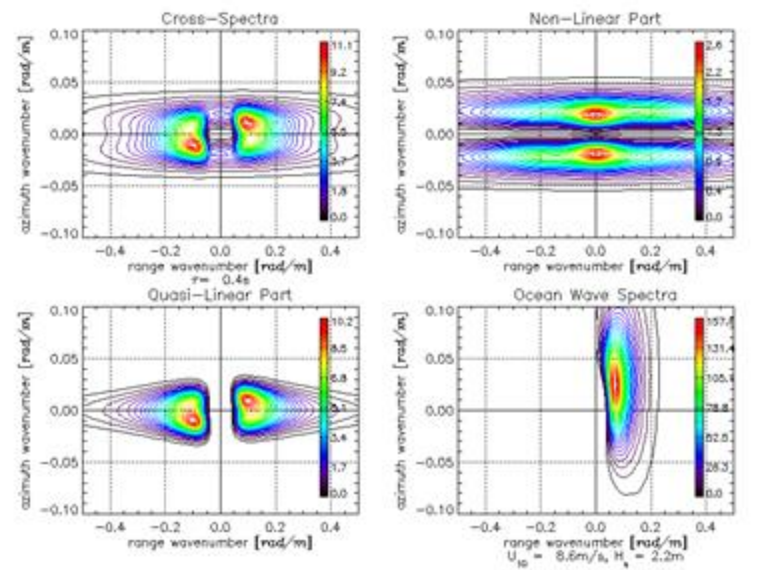

$$P(k_x,k_y) = \frac{1}{(2\pi)^2} e^{-k_y^2 \rho_{vv}(0,0)} \int\int e^{k_y^2 \rho_{vv}} L' e^{-i(k_x x + k_y y)} dx dy$$

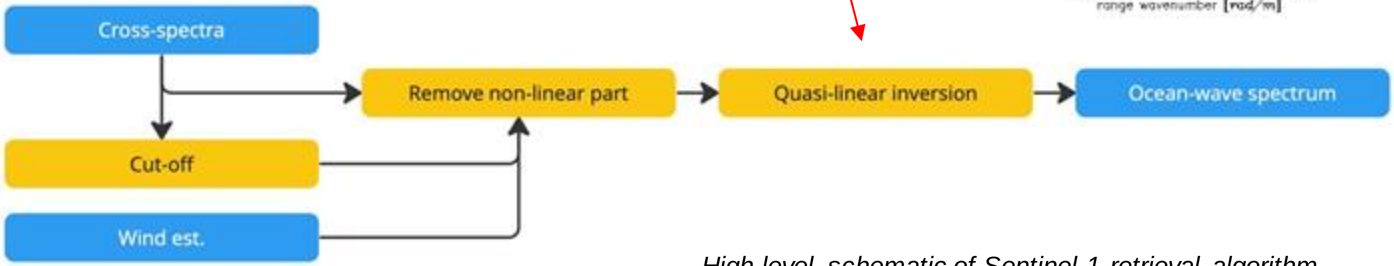

High-level schematic of Sentinel-1 retrieval algorithm

Quasi-linear inversion assessment using buoy data

- Quasi-linear inversion schemes.
- Rather well known and providing reasonable results, regardless of the intrinsic limitations.
- Focus in the analysis of SAR images acquired during varying wind and wave conditions: eg. under the presence of an atmospheric frontal system. Not so satisfactory results. (Lai and Delisi 2010)
- Next attempt, making use of the quasi-linear inversion scheme proposed originally by Krogstad et al. (1994) and used by Vachon et al (1994) –work under progress-
- Focus at detailed directional wave spectra
- Mixed sea and swell and studying the relative

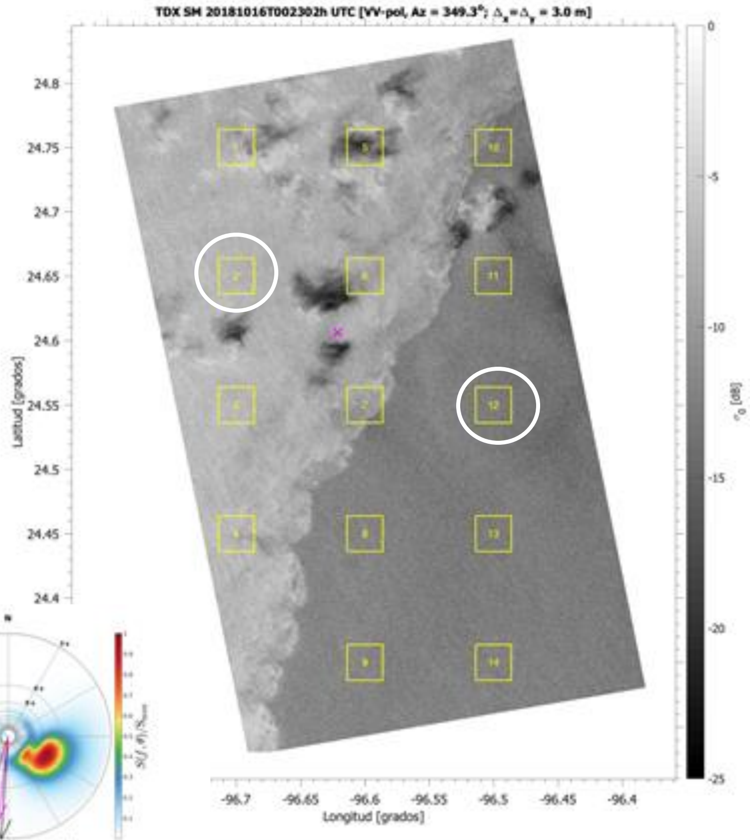

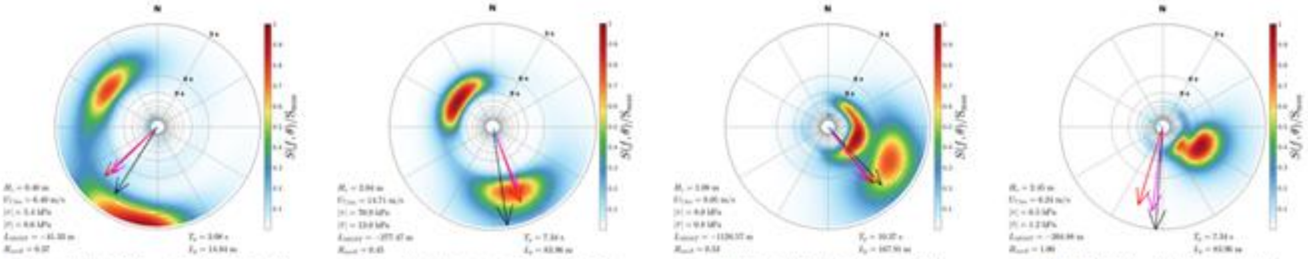

(e) Perdido 01/Ago/2018 22:07 hrs (f) Perdido 11/Nov/2018 15:22 hrs (g) ITS 03/May/2018 23:06 hrs (h) ITS 17/Apr/2018 12:49 hrs

Quasi-linear inversion assessment using buoy data

- Focus in the analysis of SAR images acquired during varying wind and wave conditions: eg. under the presence of an atmospheric frontal system. Not so satisfactory results. (Lai and Delisi 2010)

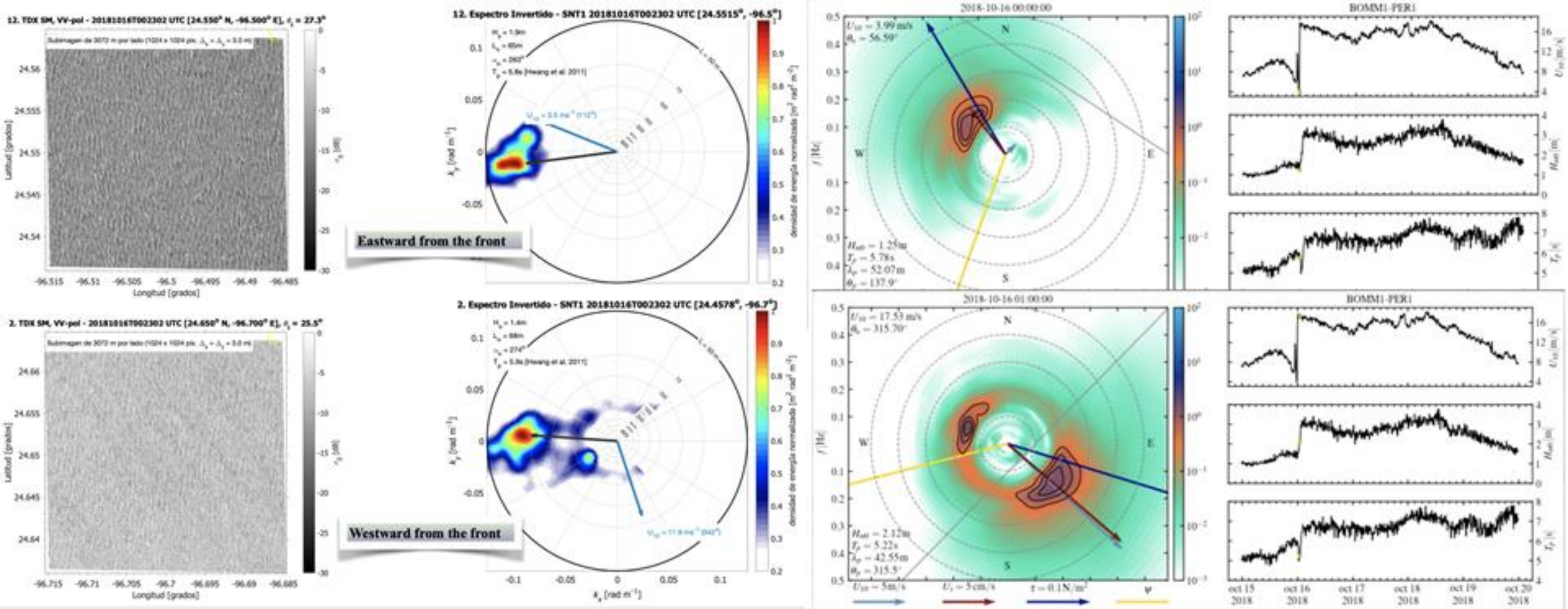

Spectral coverage

- Limited directional sensitivity due to Azimuth cut-off.
- Cut-off typically 100-200 m.

$$\lambda_c \propto \pi\sqrt{\rho_{yy}(0,0)} = \pi\frac{R}{V}\sqrt{\sigma_v^2}$$

- Wind-wave system requires parametrizations.
- Swell full recovered in low to moderate sea states.
- Issues with peak swell direction.

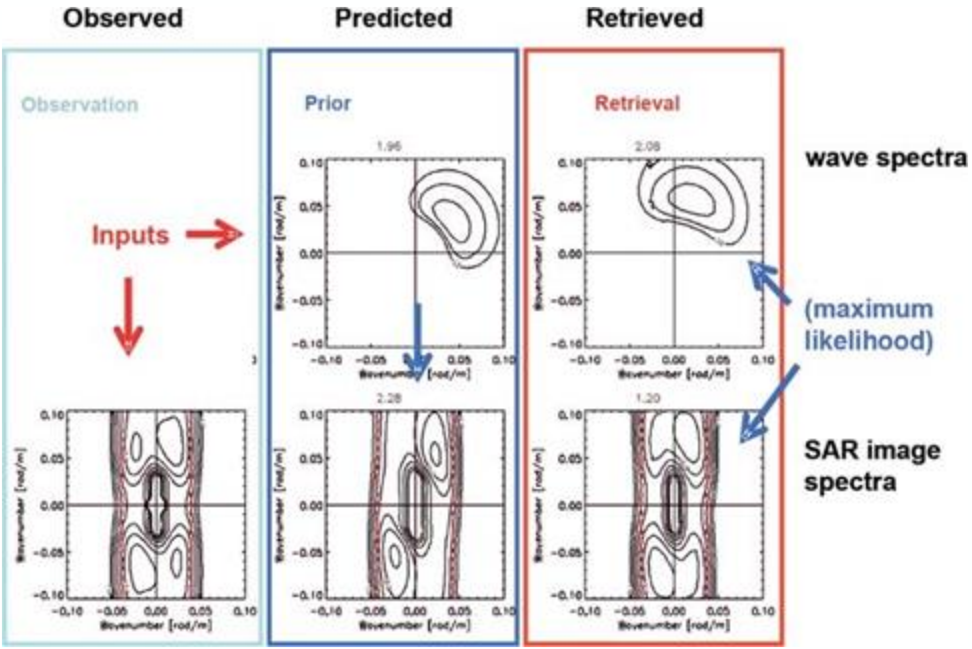

Figure from Hasselmann et al. (2012)

Known issues of the closed-form

- Limited spectral coverage.
- Time-varying geometry.
- Cut-off is affected by tilt, hydrodynamics and decorrelation.
- Cut-off estimation issues.
- Supercritical wave velocities and slopes.
- RAR response is poorly understood.

Sentinel-1 archive inconsistency

- The ESA level-2 ocean swell spectra (OSW) product is improving over time through several IPF updates.
- The improvements are not currently applied backward in time.
- This work examines the temporal consistency of the OSW product as compared to a global wave model (Smith et al., 2020 RMetS GDJ).
- The match-up criteria is within 100 km and 30 mins.
- Comparisons are done over bulk params with wave model spectra truncated using azimuth cutoff (model - S1 biases and std dev.).

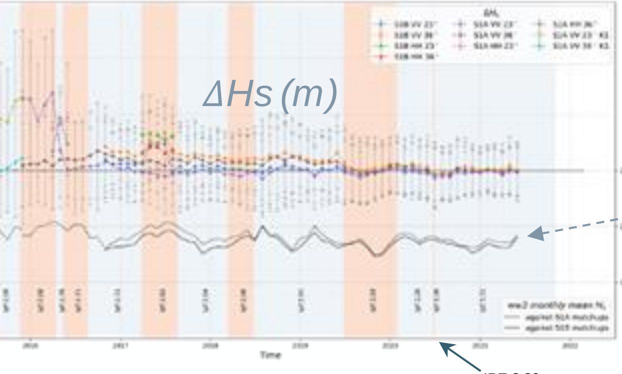

IPF 3.30

Time/IPF versions

WW3 monthly mean *Hs, Tm02, dm*

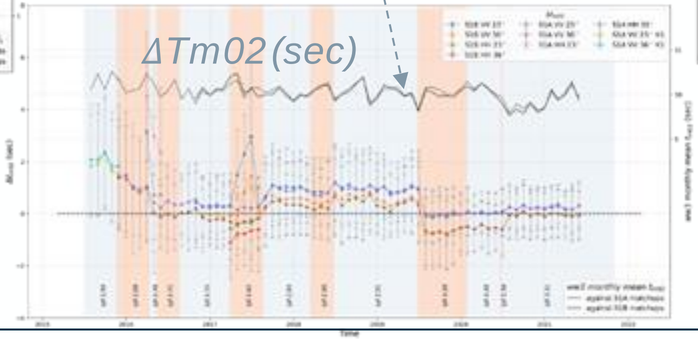

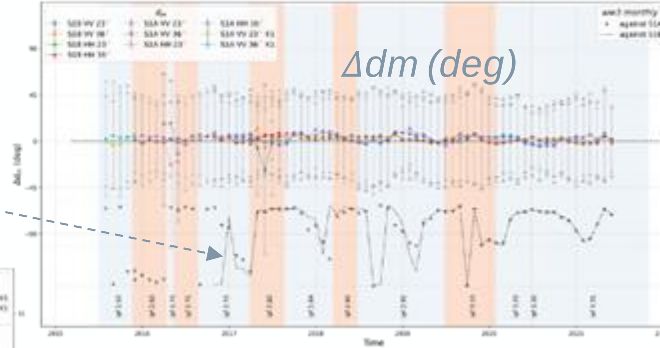

Key messages:
- Notwithstanding the azimuth cutoff limitations, the OSW product is improving in accuracy and may benefit from backward reprocessing (if feasible and economical)
- Until then, users need to be aware of the limitations

Known issues on RAR modulations

- RAR modulation damping in wind following waves.

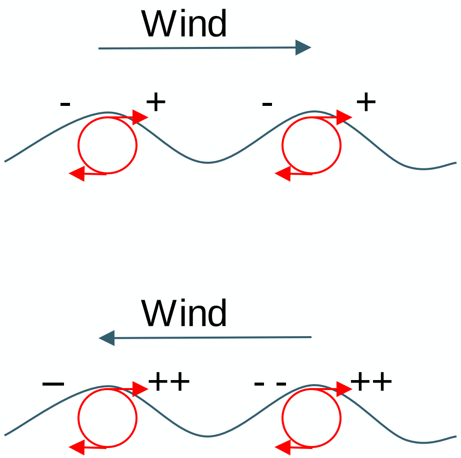

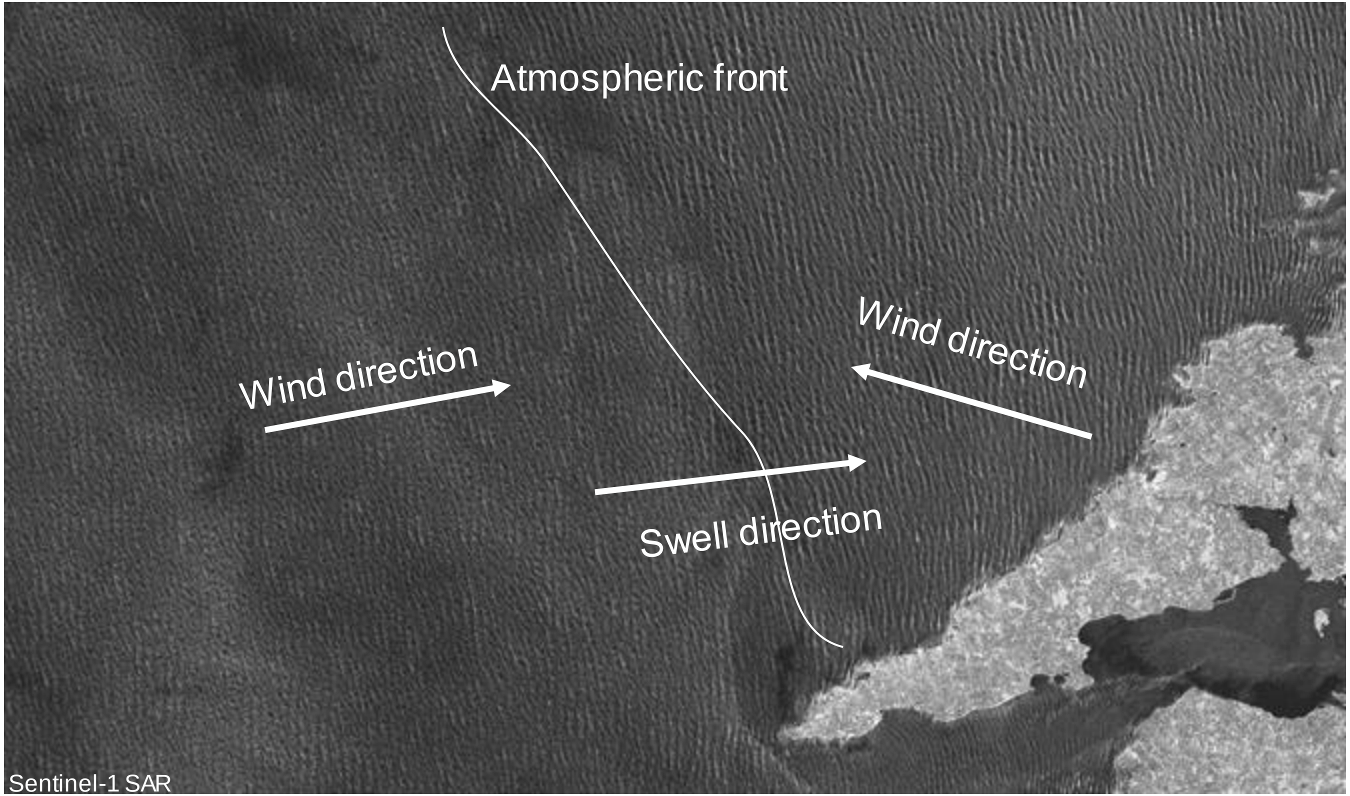

Known issues on RAR modulations

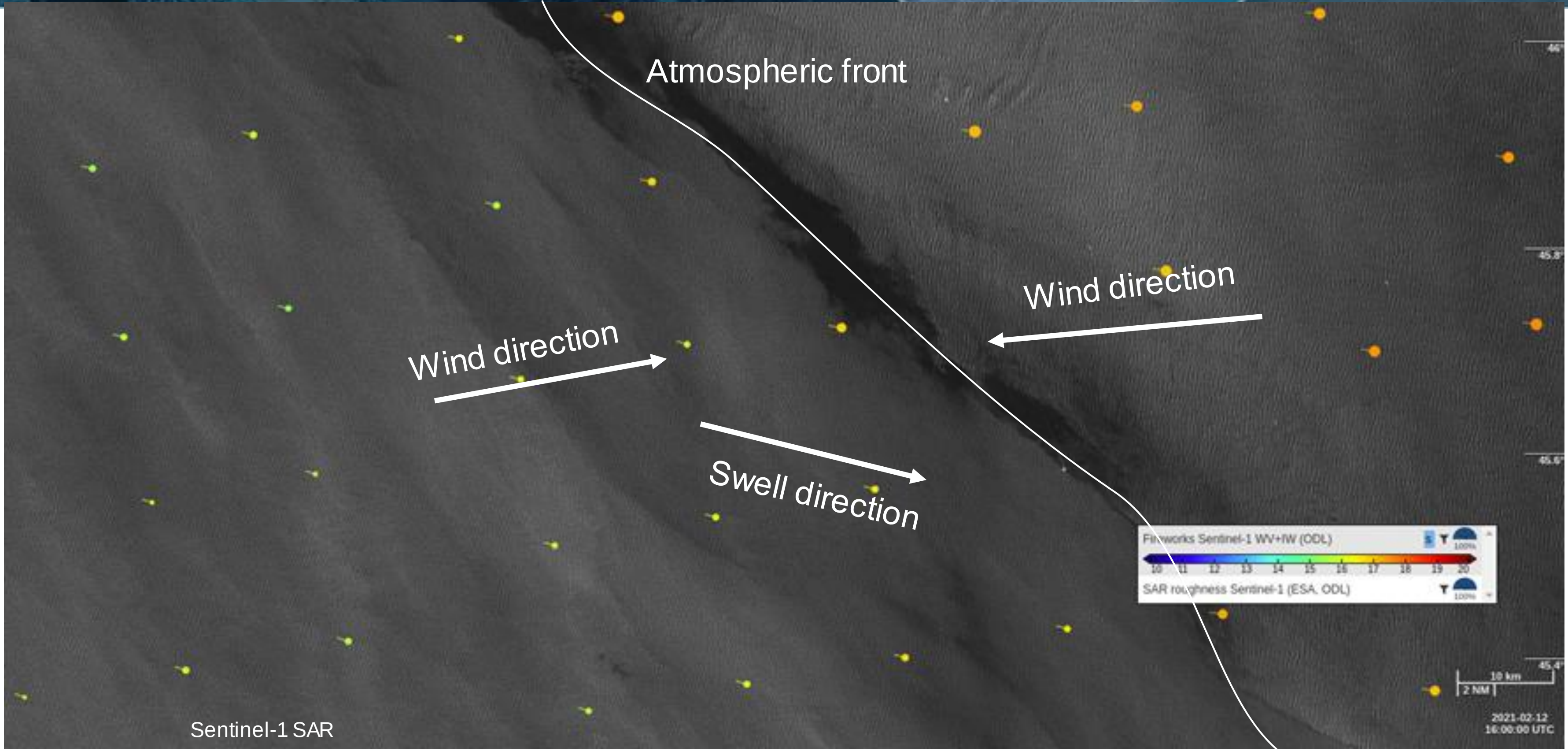

Supercritical velocities and slopes

- Most prominent at low wind-sea and monochromatic swell.
- Supercritical velocities (along-track monochromatic):

$$k_y A > \frac{V}{\omega R}$$

- Supercritical slopes (common in altimetry):

$$k_x A > \tan(\theta)$$

- Fully non-linear when d>λ/4 (Toshida et al. 2015).

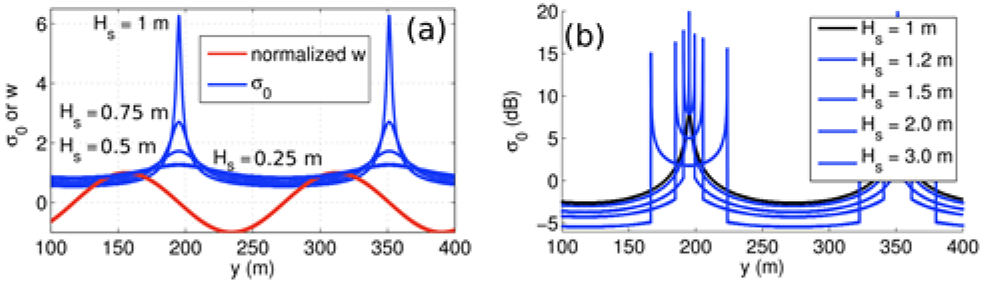

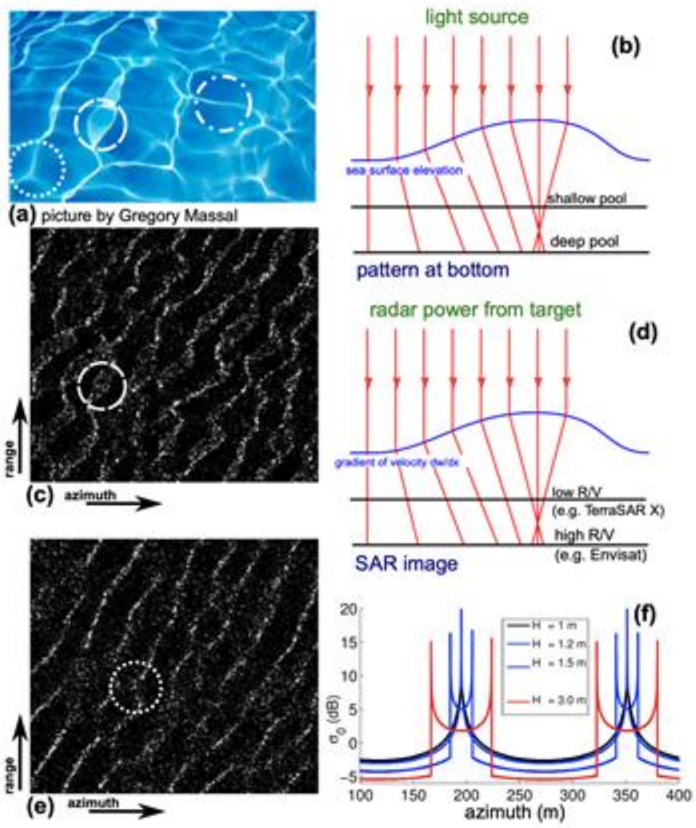

Figures from Ardhuin et al. (2015/2017).

Time-varying geometry and modulation

- Observation geometry changes during acquisition time creates significant variation of backscattered signal.
- This cross-section variation is wrongly interpreted as wave motion in cross-spectrum.
- Wave direction of propagation can be inverted for sufficiently long wave (with negative azimuth wavenumber).

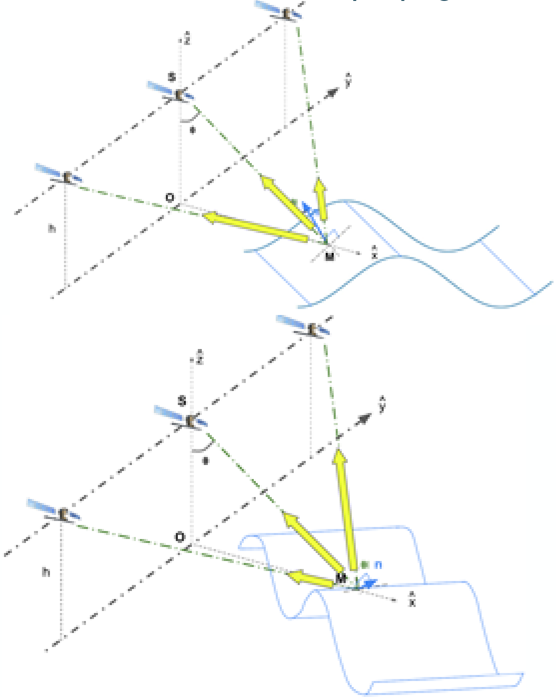

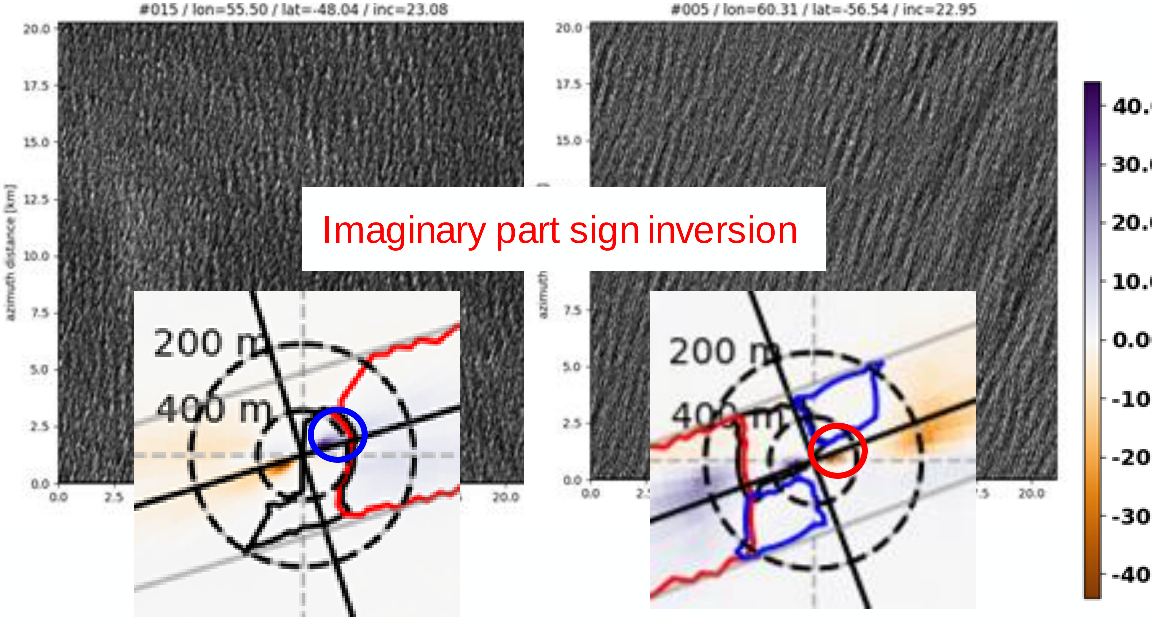

- This phenomenon has to be added to the close-form equation

Mean impact on cross spectral phase

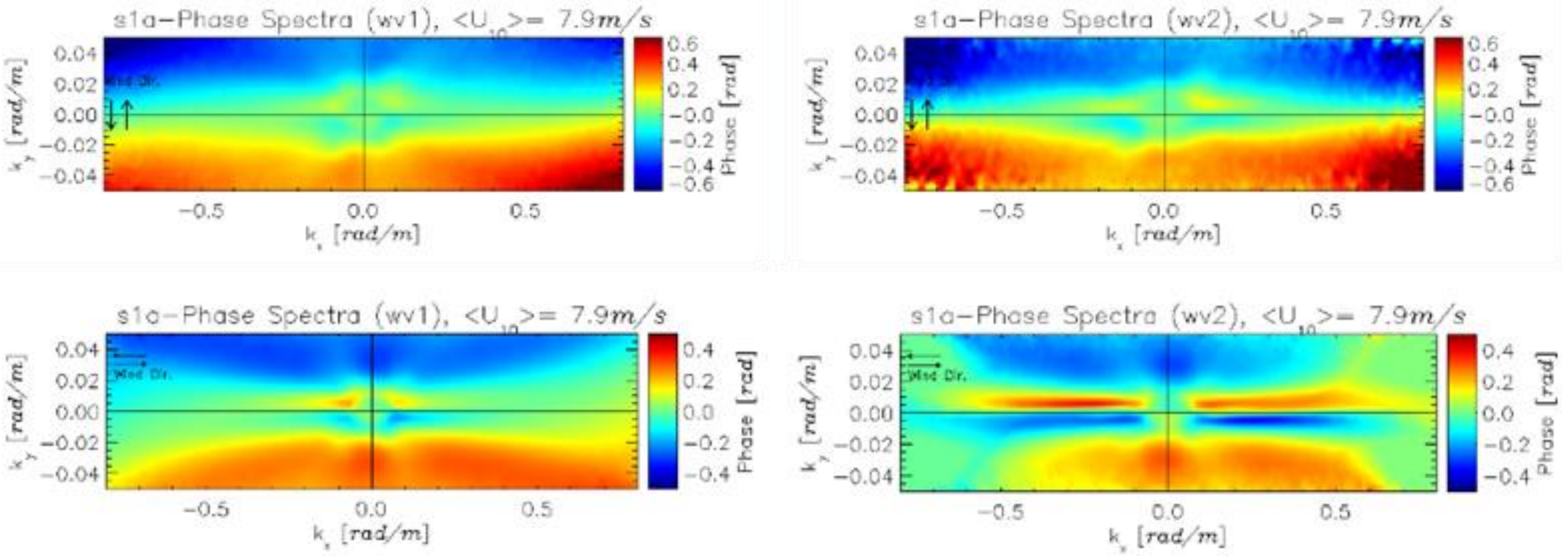

Mean phase spectra for ±azimuth (upper) and ±range (lower) winds.
Left: wv1, Right: wv2. Ocean data.

Neural-network approaches

- Decomposition of spectrum (CWAVE, Schulz-Stellenfleth et al. 2005/2007).
- Estimation of integral wave parameters using (step-wise) regression.

- ‘Engineered’ machine learning for Sentinel-1 (Stopa & Mouche, 2017; Wang et al. 2018).
- Deep-learning approaches involving the full spectrum (Quach et al. 2021).

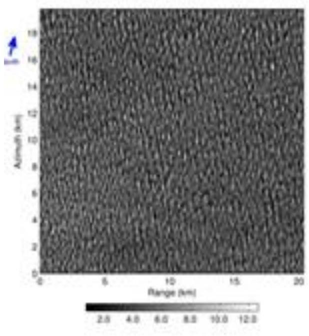
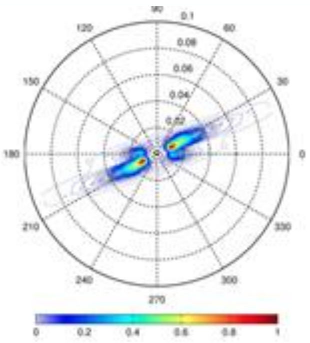
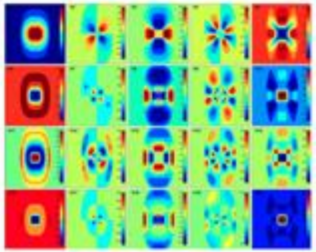
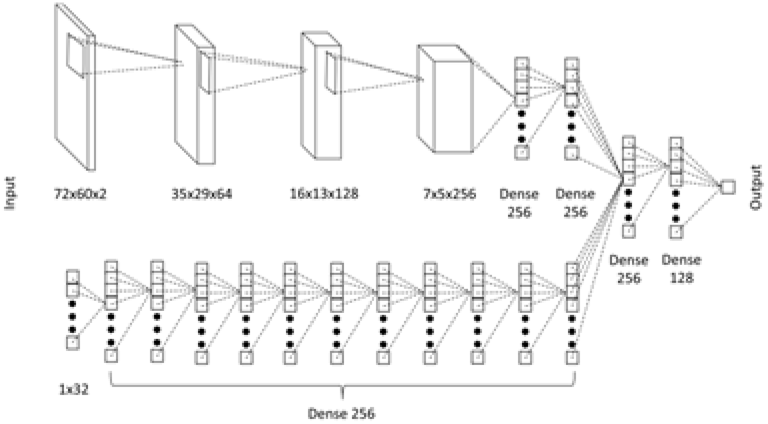

Figures from Quach et al. (2019)

Deep-learning for sea-state retrieval

- Wind-sea related to present/recent winds: complex non-linearities and partially or totally removed from the SAR spectral signature (azimuthal cut-off).
- DNN method to estimate the wind-sea Hs from S1 with a data driven approach applied to either 2 estimations of the wind sea Hs variable:
  - - WW3 wind sea partition,
  - - wind sea component of the wave spectrum (based on Cg and wind vector)
- Dependence to input features can be estimated overall and for various conditions:Skewness, Azimuth cutoff, various IMACS of longer wavelength for higher wind speeds.

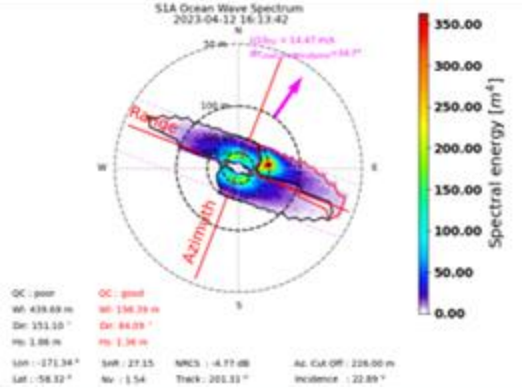

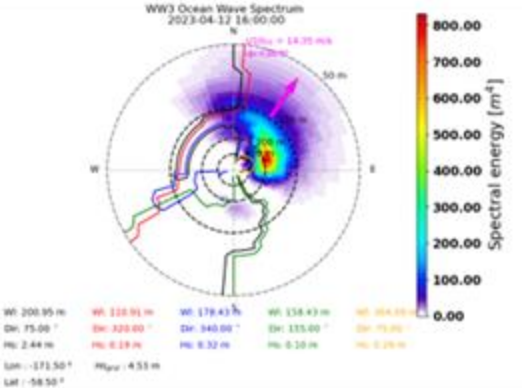

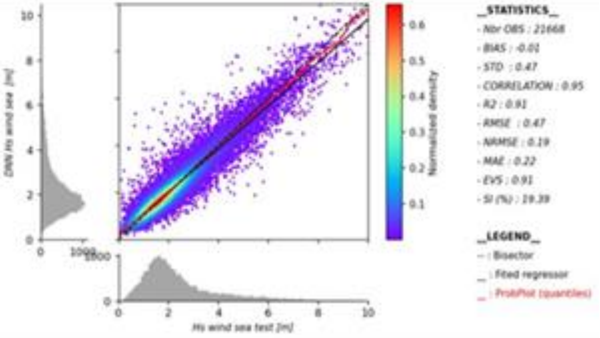

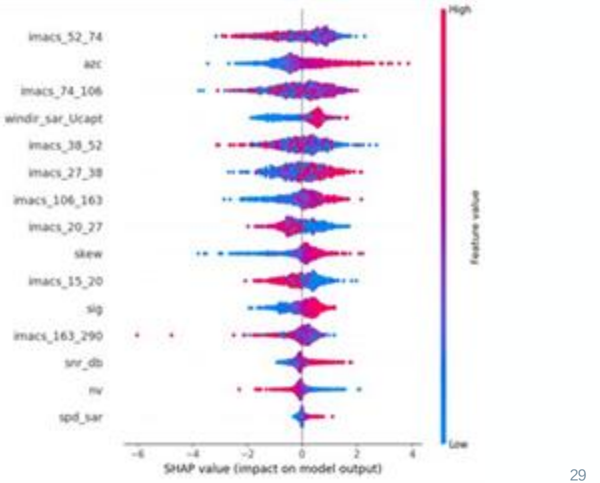

LSTM to transform image spectra to wave spectra

- Sentinel-1 IW image spectra in the wind-wave dominant Baltic Sea; WAM based NORA3 wave spectra.
- 60k collocations; Vanilla LSTM recurrent neural network (~20k trainable parameters).
- Training objective is to minimize RMSE and maximize correlation.
- Validation on 7749 data points/spectra.
- Majority of spectra to spectra correlations are above 0.9.
- Correlations by frequency bins accurate; RMSE low for higher frequencies.
- For H_S calculated from spectra $r = 0.91$ and RMSE 0.3 m. For T_{m01} $r = 0.84$ and RMSE 0.5 s.

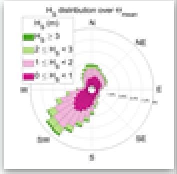

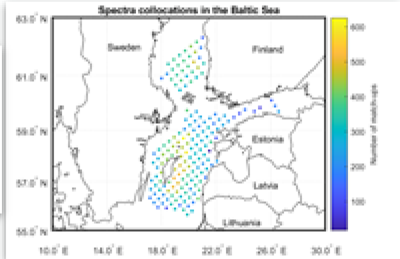

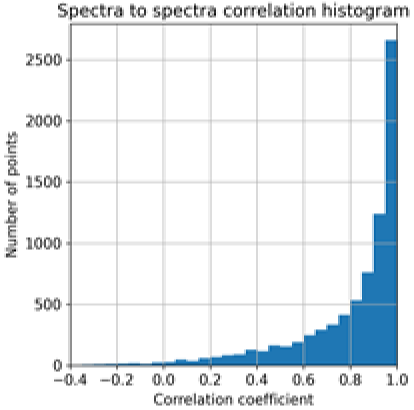

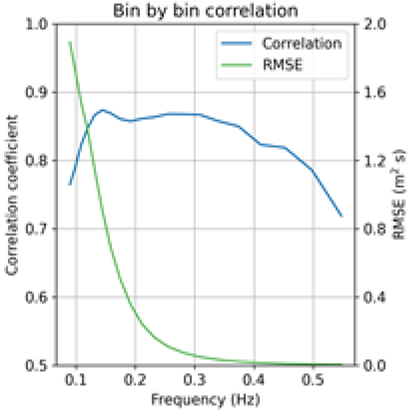

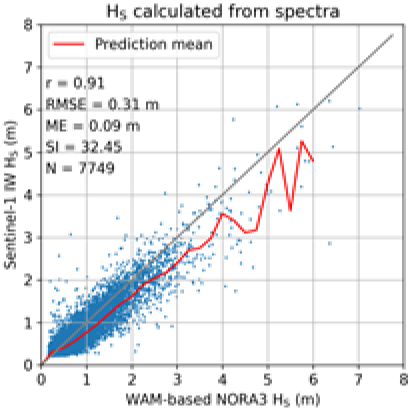

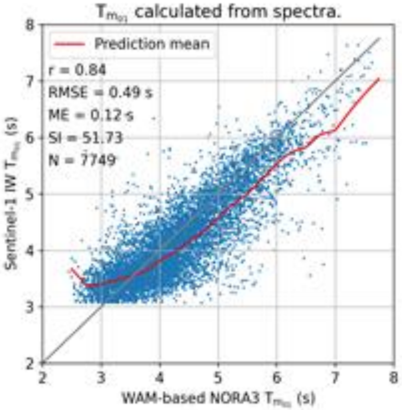

SeaStaR (SAR Sea State Retrieval) empirical algorithm

Algorithm opportunities and implementation: SeaStaR (SAR Sea State Retrieval) new empirical algorithm

- Processing parameters output in form of fields (raster, e.g. one S1-IW with 3 km raster – ca. 5000 values/image-ID)
- Series of integrated sea state parameters (8 parameters: SWH, Swell SW1, SW2, Windsea; Periods Tm0, Tm1, Tm2, Windsea-Period)
- Algorithm realized in Sea State Processor for daily Near Real Time (NRT) services (uniform modular architecture for different satellites)

Algorithm innovation

- Combination of classical approach using linear regression with machine learning (CWAVE approach + support vector machine SVM)
- Five types of SAR features: NRCS statistics, geophysical (wind), GLCM, spectral parameters + new introduced features, CWAVE
- Method applied for processing Level-1 (L1) products for different satellites (modes):
  - Sentinel-1 Wave Mode (S1-WV), SLC
  - Sentinel-1 Interferometric Wide Swath Mode (S1-IW), GRD
  - Sentinel-1 Extra Wide (S1-EW), GRD
  - TerraSAR-X StripMap (TS-X SM), GRD

Algorithm tasks

- Artefact (ships, fronts, etc.), SAR processing errors and antenna beam pattern filtering, denoising
- Features extraction, feature error analysis
- Model functions
- Control results, filtering, flagging
- Map Client

Achieved RMSE total significant wave height SWH (m) worldwide:

	S1-WV	S1-IW	S1-EW	TS-X SM
Compared to model	0.25	0.43	0.48	0.37
Compared to buoys	0.41	0.49	N/A	N/A

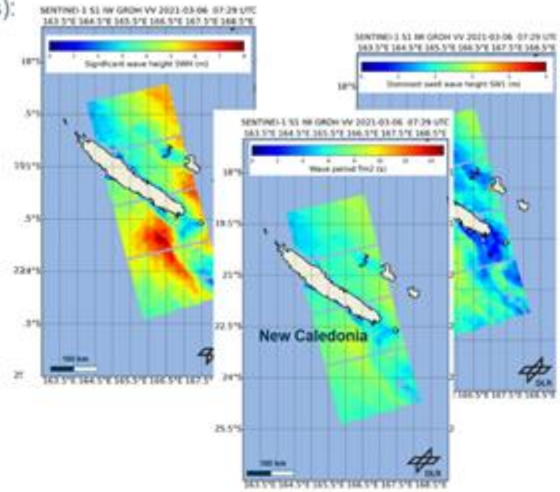

Sea state fields examples: processing S1-IW with 5 km raster (ca. 1500 values/image): 4 ID-products cover ca. 200 km × 900 km

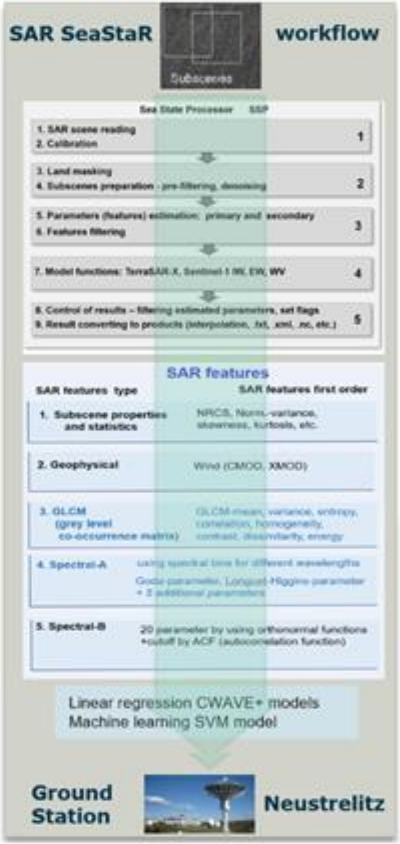

SeaStaR (SAR Sea State Retrieval) empirical algorithm

DLR finished validation SWH and Tm2 for S1-IW archive 2020 in frame of ESA-SARWAVE (ca. 12,000 scenes, 5 km processing raster) with model WFWAN (CMEMS) and buoys

- -55°<LAT<60° (avoiding ice coverage)
- 10 km from land, max 10 km from buoys
- Max time gap measurements 3 h

SARWAVE validation dataset S1-IW 2020

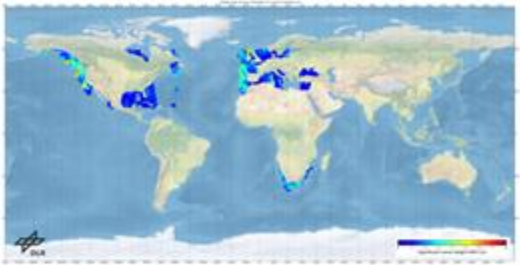

Model: ca. 8,000,000 collocations

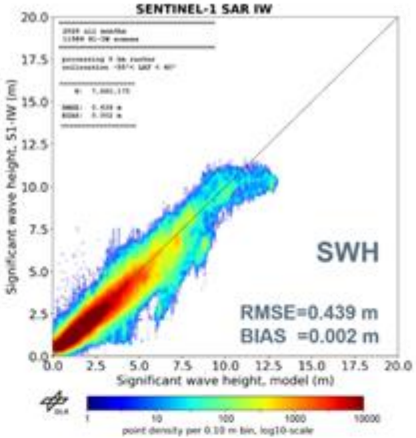

Buoys: ca. 26,000 collocations, 145 buoys worldwide

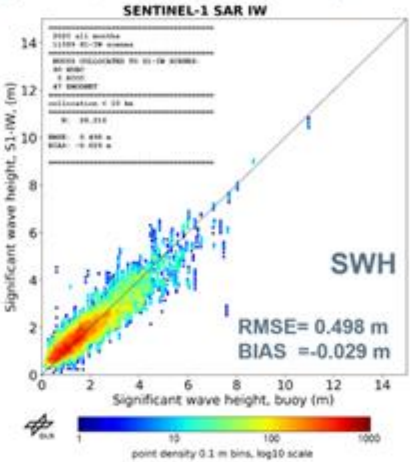

Example time series 2020-01, buoy EMODNET-1043928

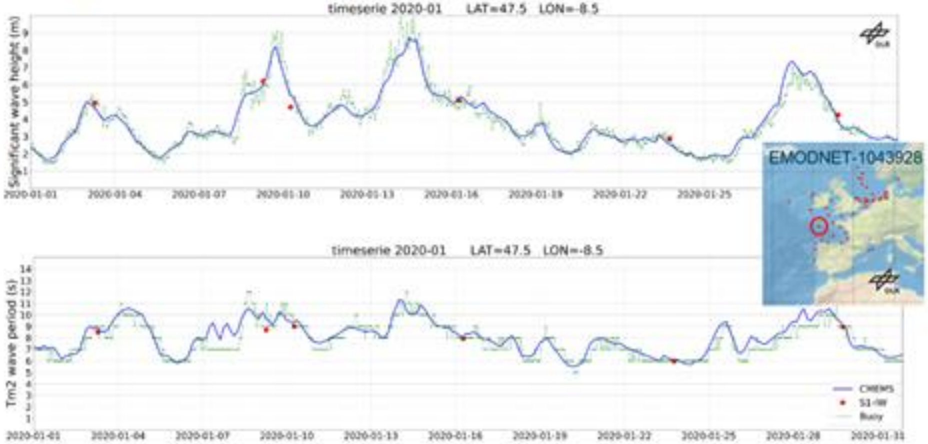

Pleskachevsky, A., Tings, B., Jacobsen, S., 2022,
Multiparametric Sea State Fields from Synthetic Aperture Radar for Maritime Situational Awareness.
Remote Sensing of Environment, Vol. 280, Oct. 2022, 113200, Open access

Limitations of neural-network approaches

- Current neural-network approaches only retrieve integrated parameters.
- Filters applied to capture various scales are not causal.
- Not all parameters from side-looking SARs are fully exploited.
- Input parameters such as the cut-off suffer from estimation issues.

- Neural networks still suffer from the single line-of-sight of Sentinel-1.
- If available → multi-sensor constraints.
- Exploit improved ocean-wave models.

SAR Swell tracking

Firework analysis : Principle

- Extraction of swell systems parameters from wave spectra level2 products.
- Backward propagation to identify the swell origin (Storm source).
- Identification of all swell observations relative to a given Storm source.
- Determination of the propagation path by forward and backward propagation between observations (using deep water waves dispersion relation).

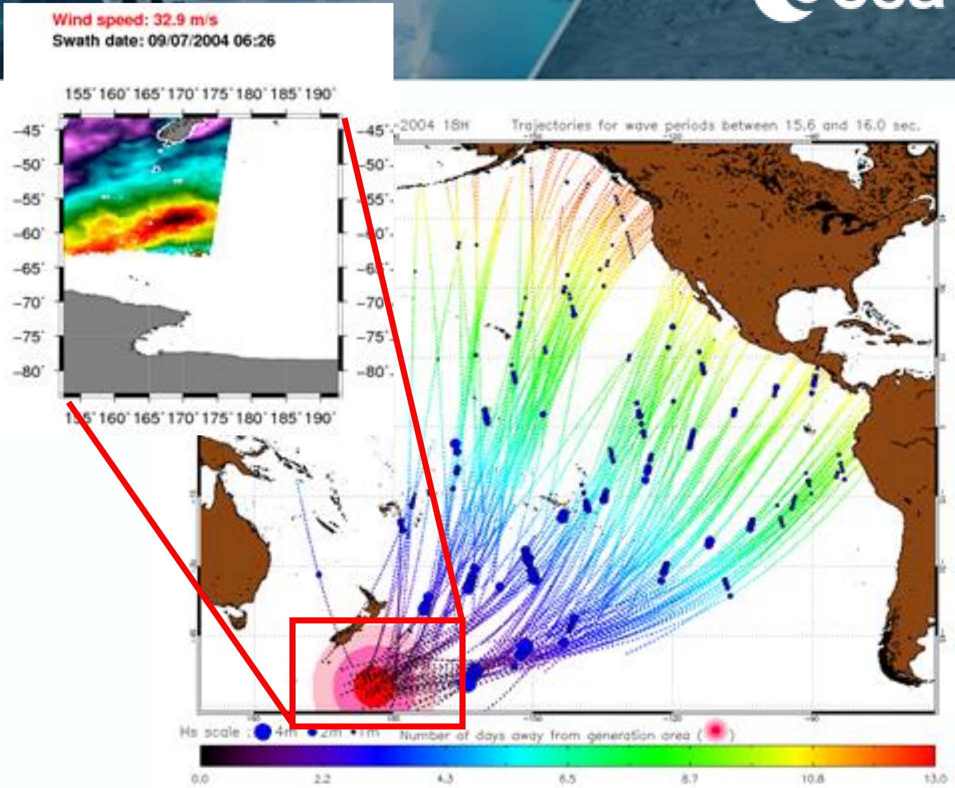

Propagation of 15-16s swell from July 8 to July 20, 2004

Envisat ASAR wave mode

Sentinel-1 Wave Mode Swell tracking

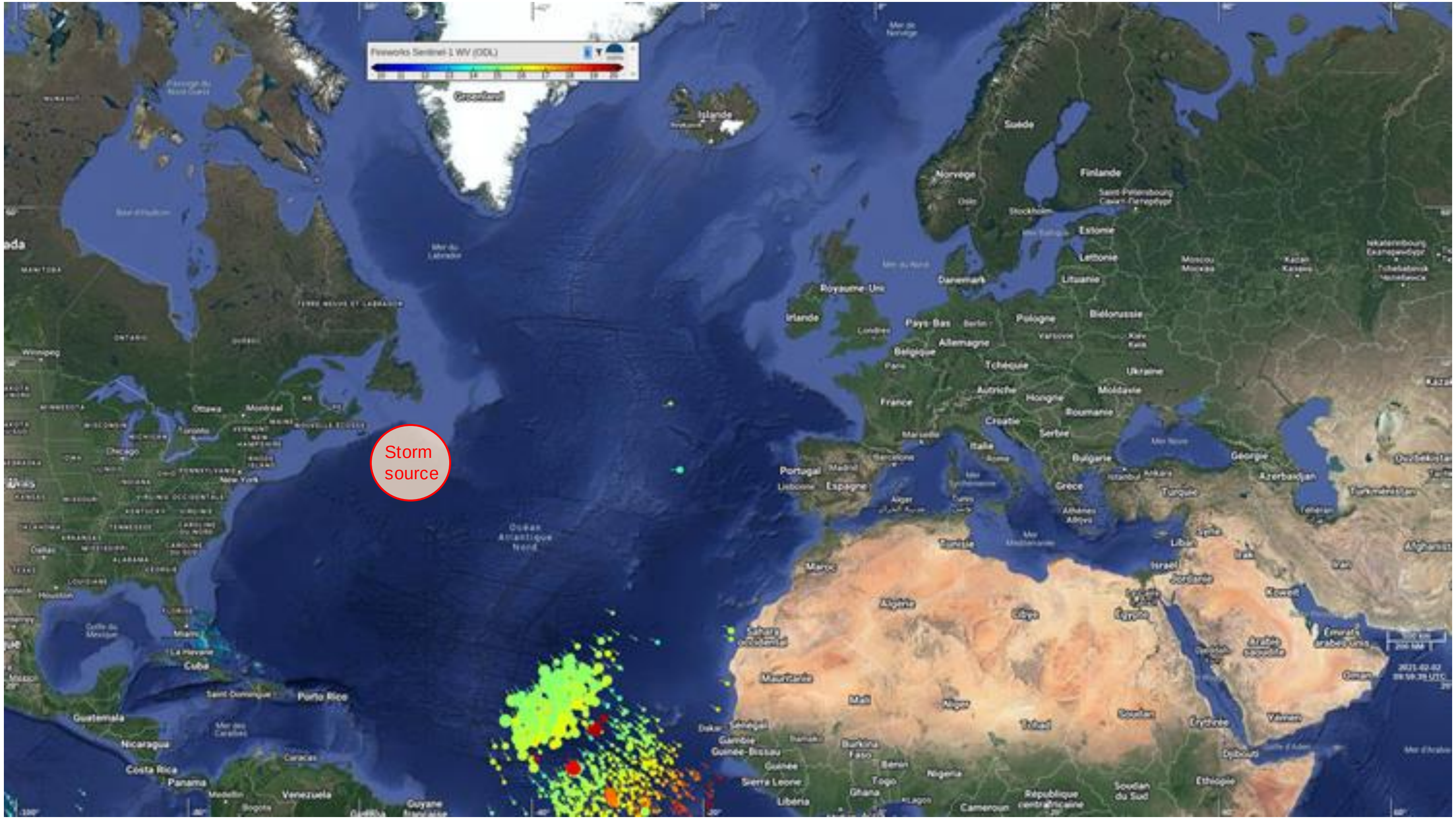

Sentinel-1 WV+SWIM Swell tracking

esa

SWIM
Wave
scatterometer
L2S wave
spectra
available
publicly in NRT

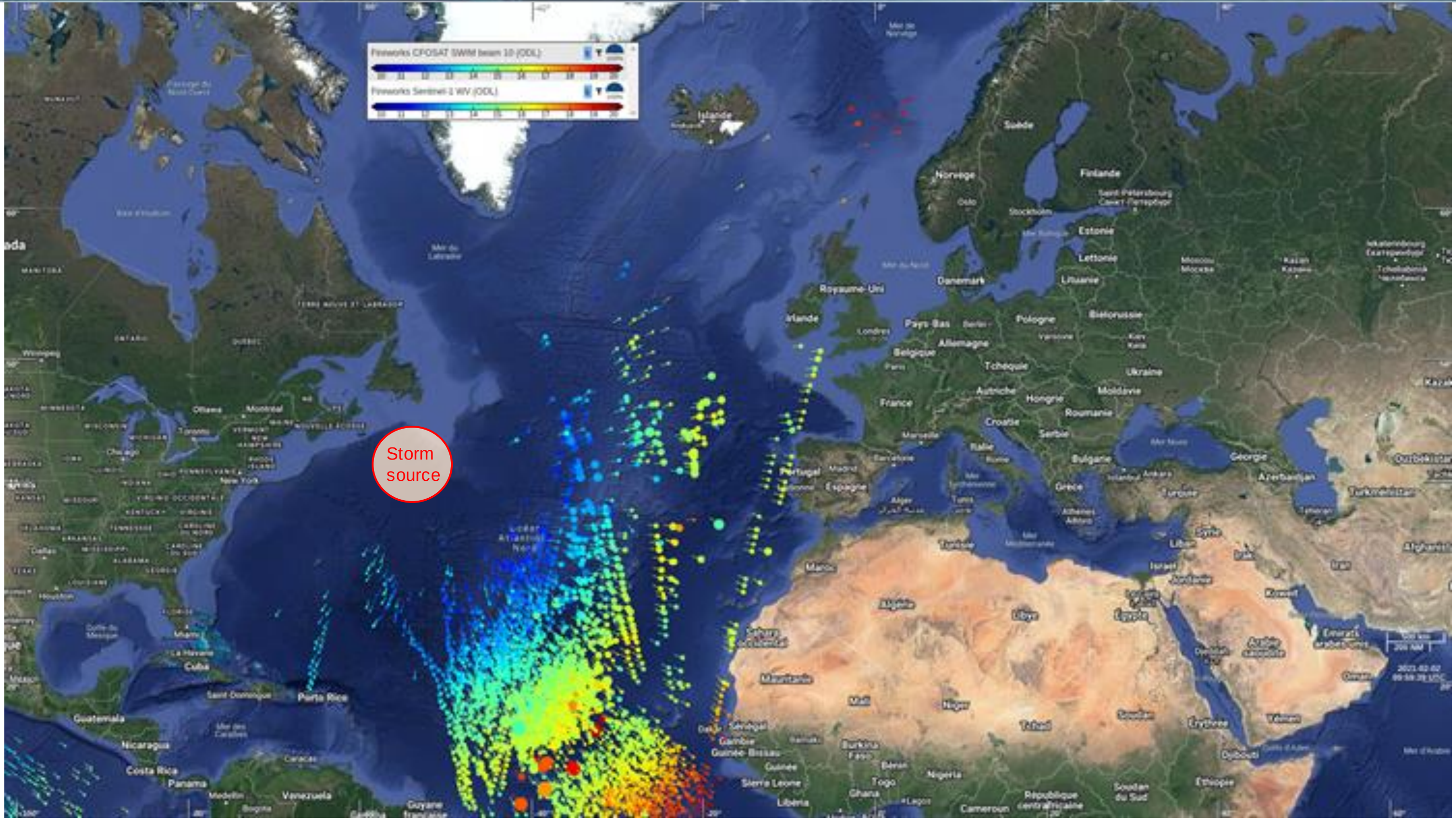

Sentinel-1 WV+SWIM+IW Swell tracking

IW cross
spectra imag.

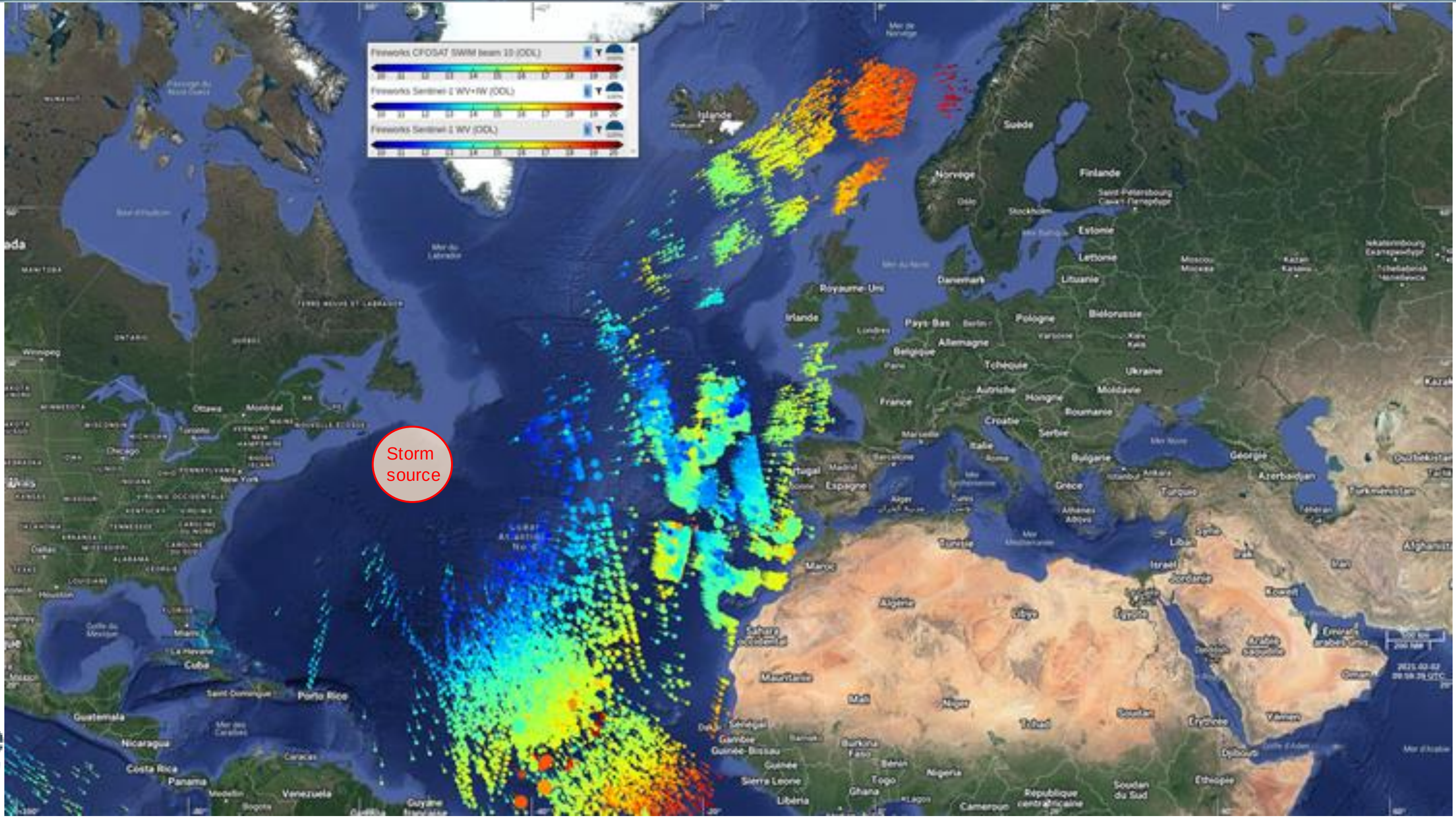

sarwave

Tropical cyclones generated waves

Results on TC Larry

These polar plots are wave roses, each point is an acquisition from the map, the distance to center is the wavelength, the polar angle is the direction of propagation with respect to the direction of the tropical cyclone

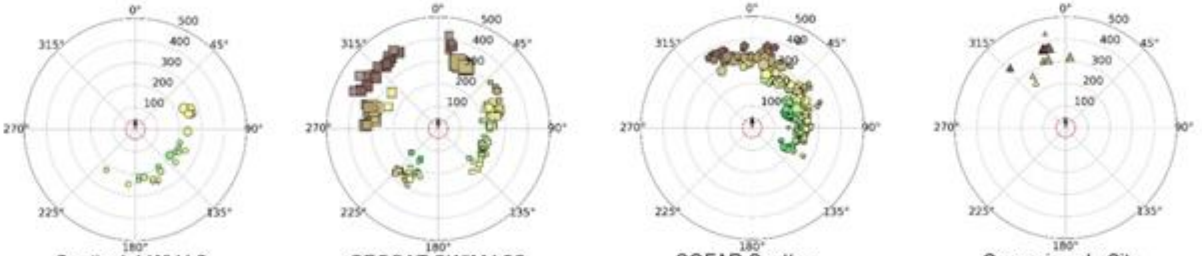

The result is a description of the wavelength of emitted waves as function of the direction of propagation

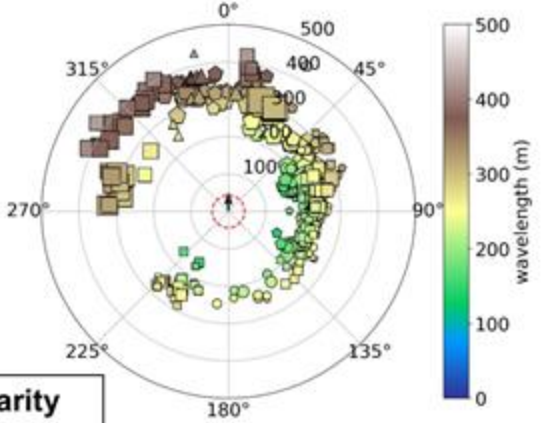

Multi-sensor wave rose

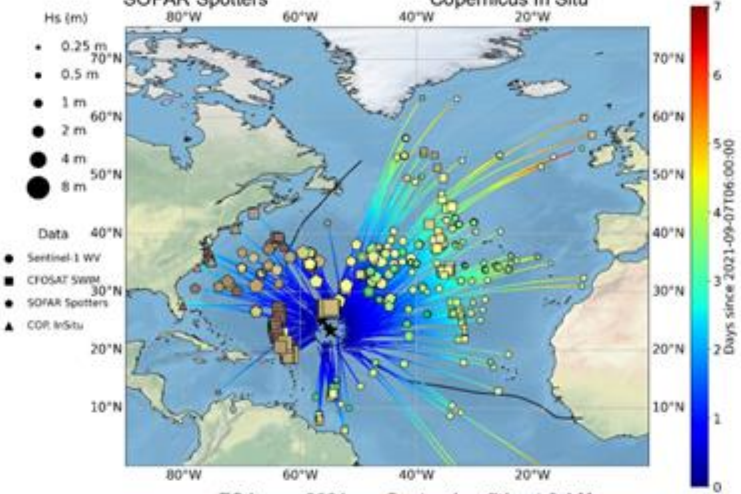

TC Larry, 2021, on September 7th, at 6 AM

Good complementarity
Good consistency
between different sensors

Such an analysis is performed for tropical cyclones between 2015 and 2021 —> So called TC waves product

Assimilation into models

- The assimilation of partitions wavenumbers (Kx-Ky) : complementary use of SAR (150-800m wavelength) and SWIM (60-500m of wavelengths).

cyclone Freddy Feb.2023

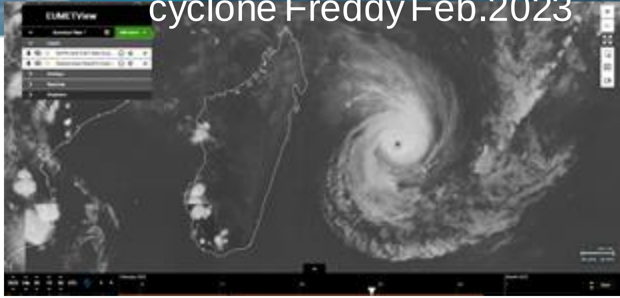

example during cyclone Freddy nearby the cyclone eye

with assimilation (SAR+SWIM)

without assimilation

difference w/wo assimilation

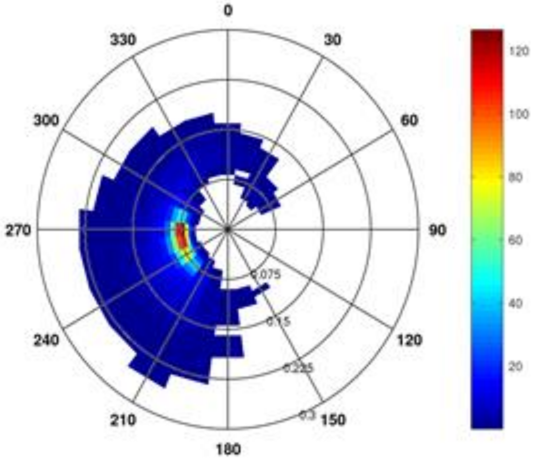

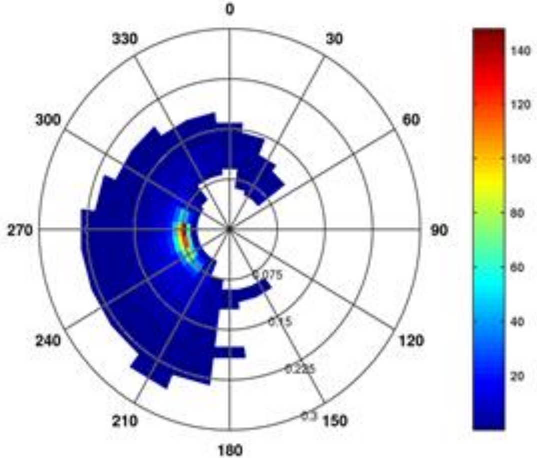

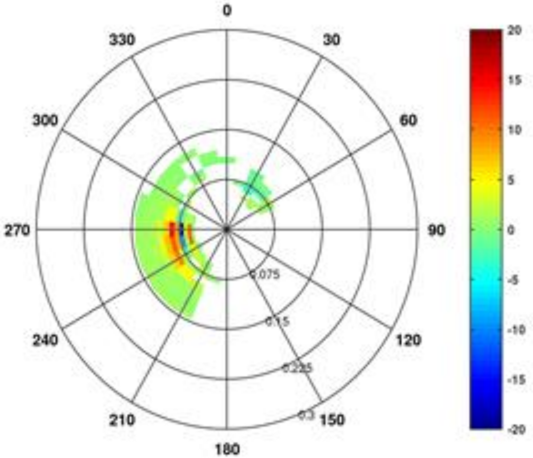

relevance of the assimilation of SAR and SWIM in Southern Ocean (February 2023)

Assimilation SWIM+SAR

without

Bias maps of SWH (max. range 120cm)

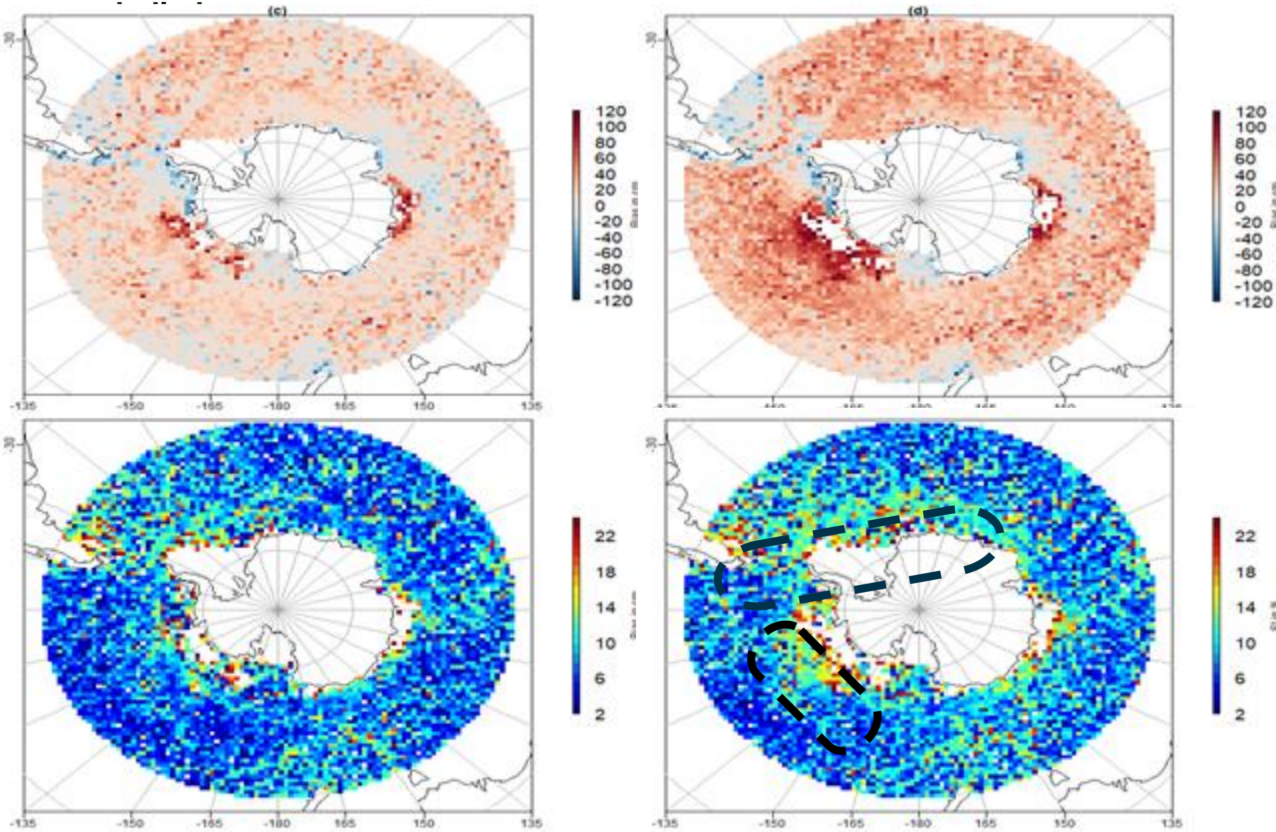

Remarkable reduction of SWH bias when using the assimilation of SAR and SWIM partitions wavenumbers.

Significant improvement of scatter index in the MIZ and swell track.

validation with independent altimeters SWH average difference of SWH between the assimilation of SWIM and the assimilation of SAR (May-Aug 2020)

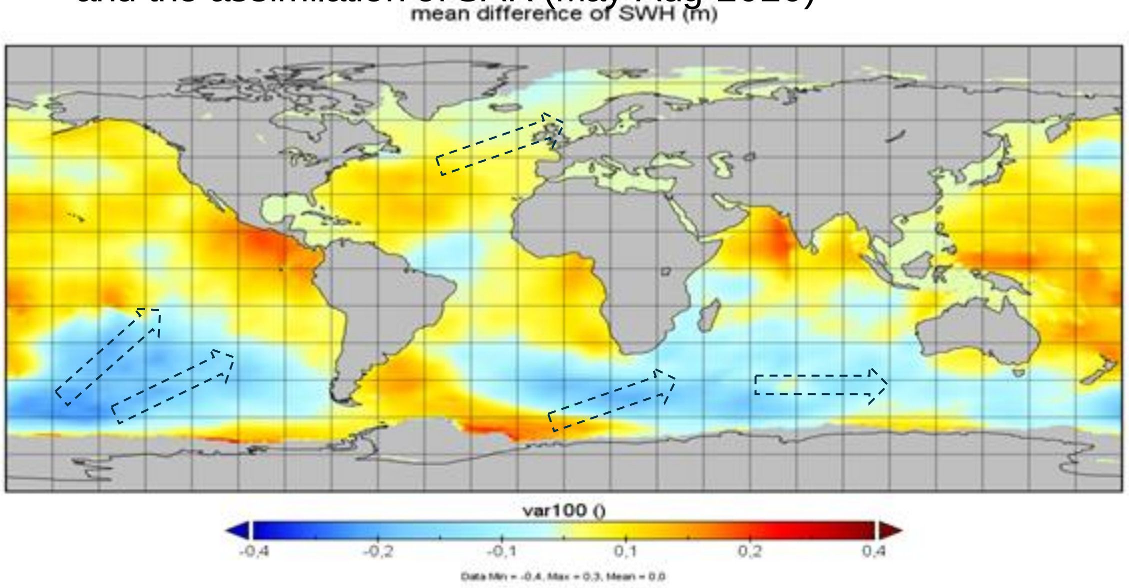

we clearly show the better scaling of wave energy/peak period induced by the assimilation of SWIM for smaller wavelengths in southern storms (blue color).

the red color indicates that SWIM is missing correction for longer waves (~>500 m), and where SAR is highly skilled.

North and North-East Atlantic is mostly affected by the assimilation of SWIM.

blue color stand for overestimation of SAR assimilation, while red color stand for overestimation of SWIM

Wave observations in sea ice

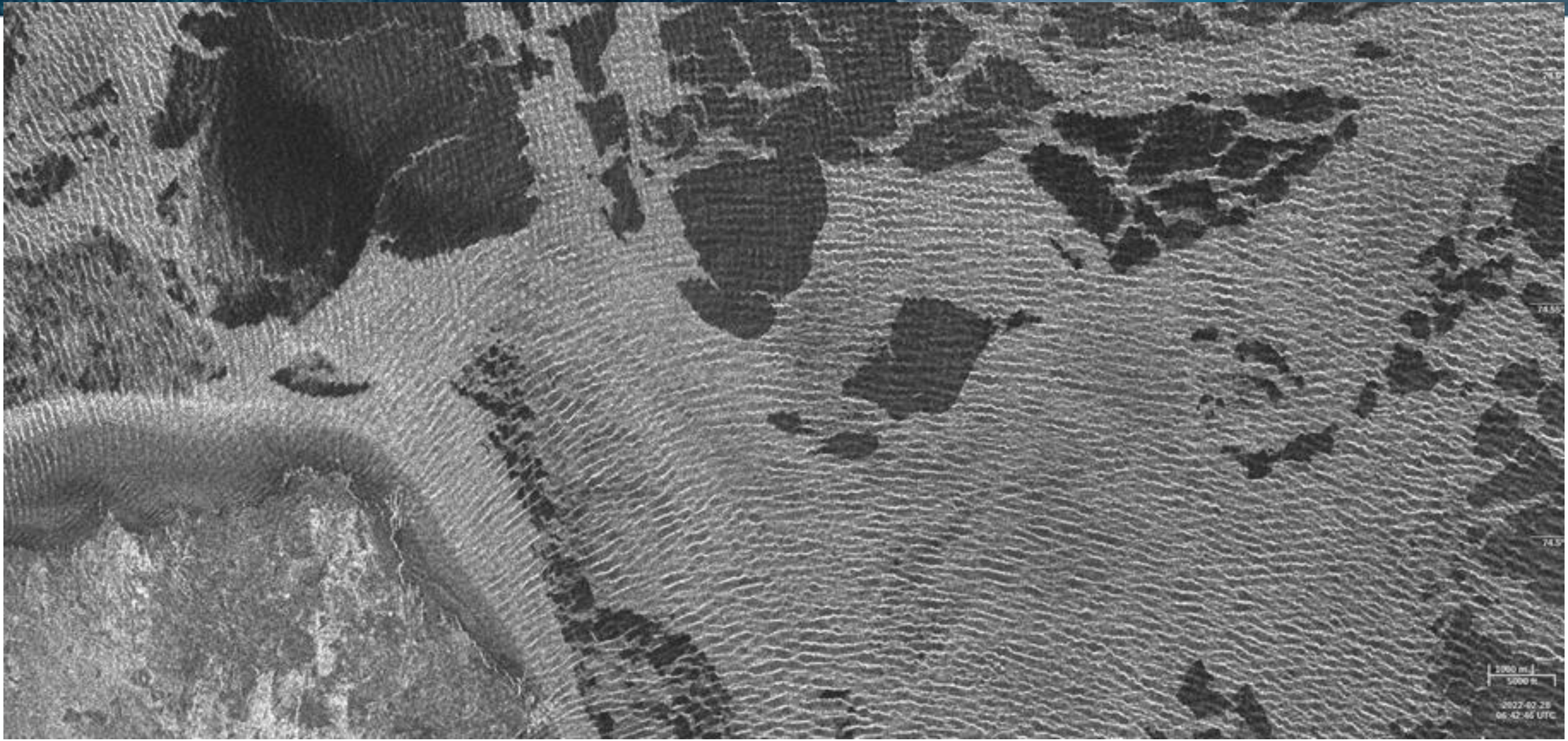

Wave observations in sea ice

Figures from Ardhuin et al. (2015/2017)

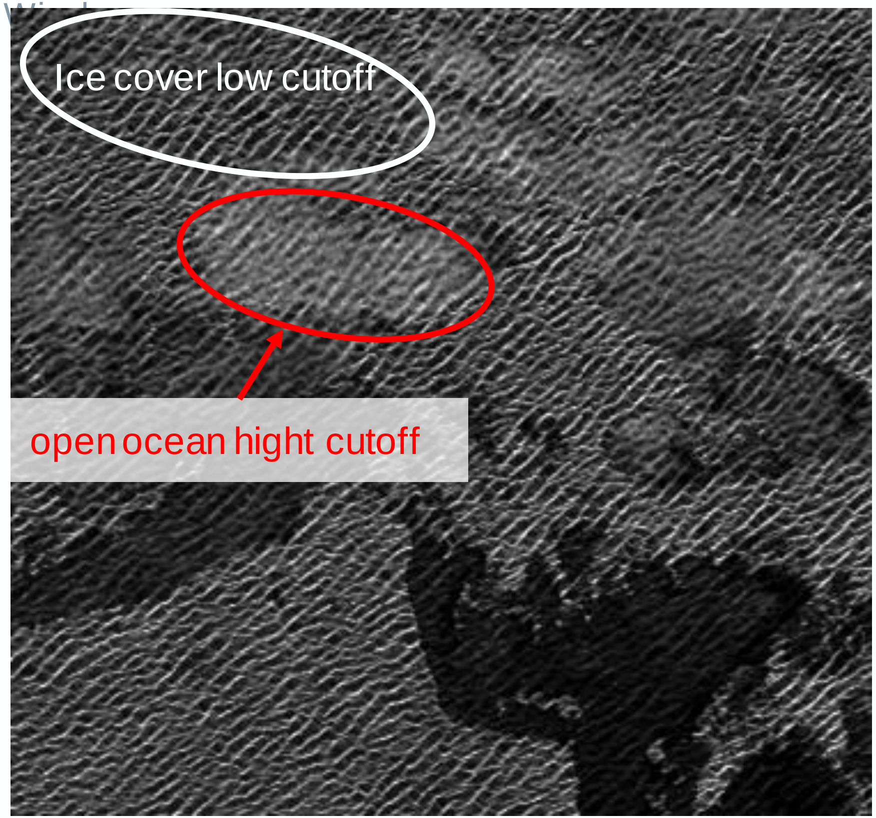

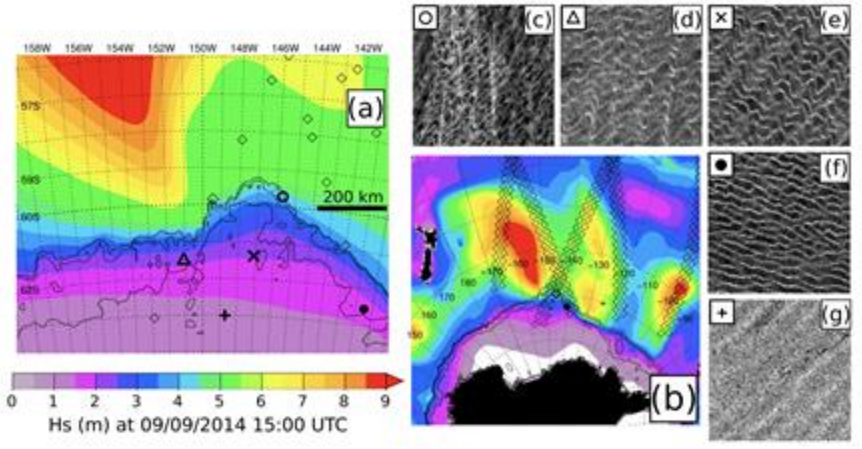

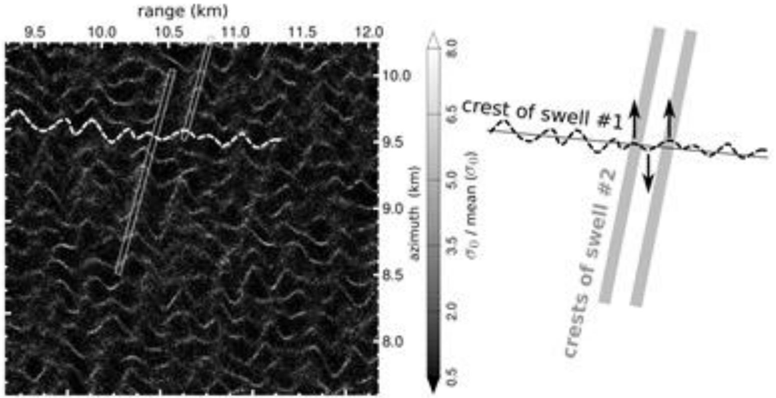

Wave observations in sea ice

- Iceberg reflections.

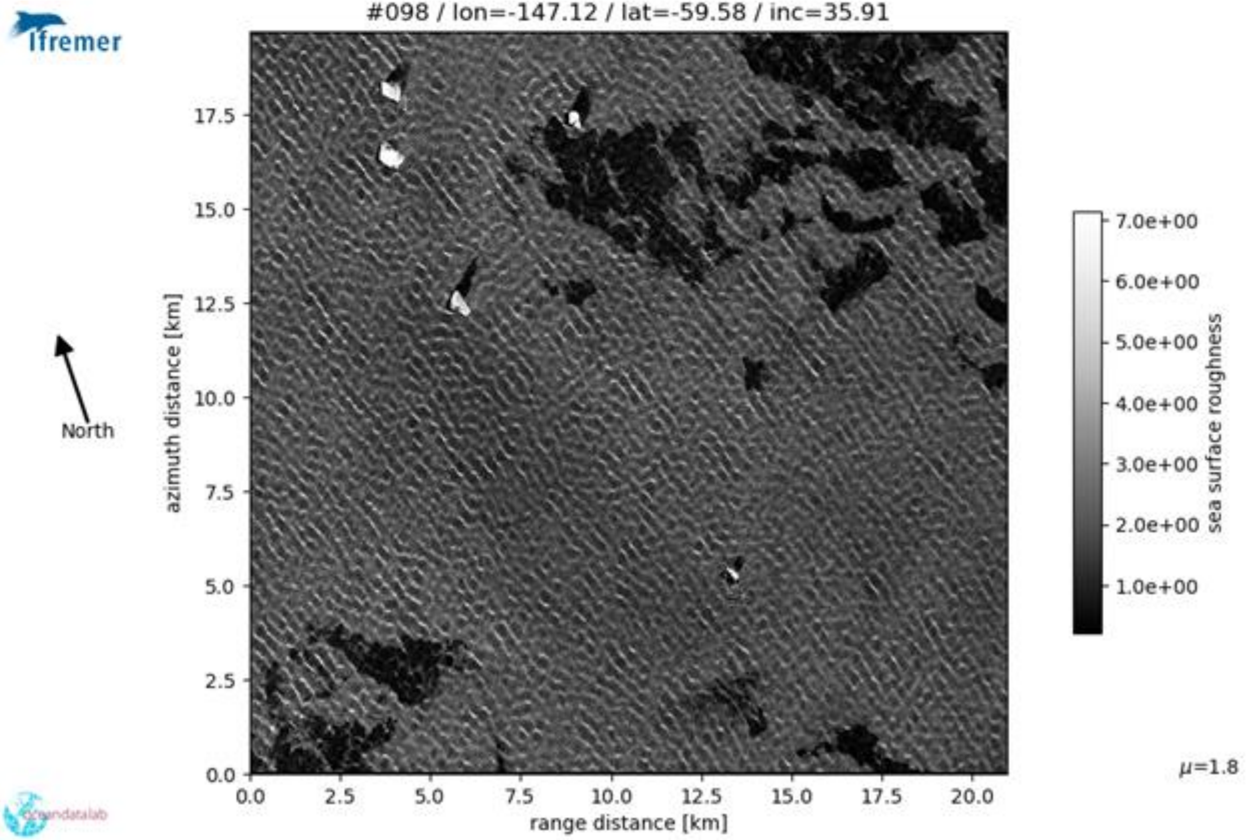

Synergies in sea ice

- SAR, SAR altimetry, XTI, optical, lidar.

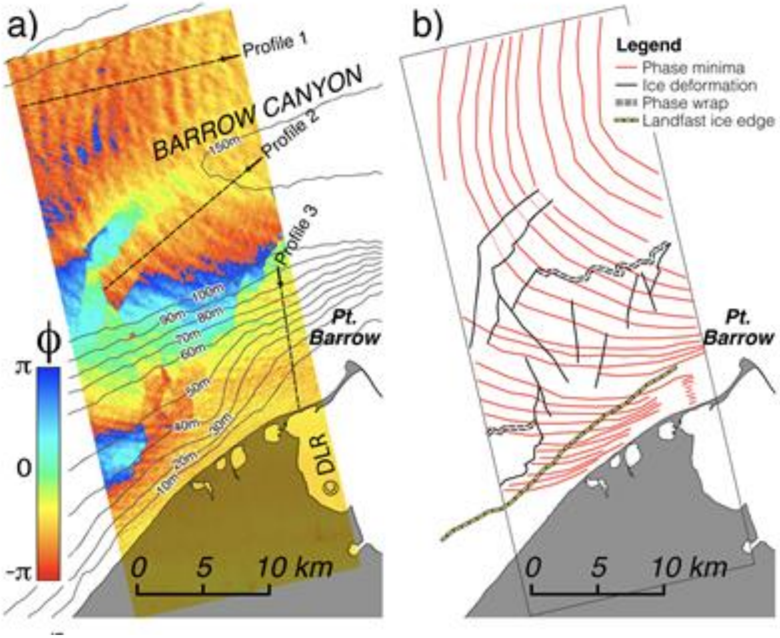

From Mahoney et al. (2016)

From Collard et al. (2022)

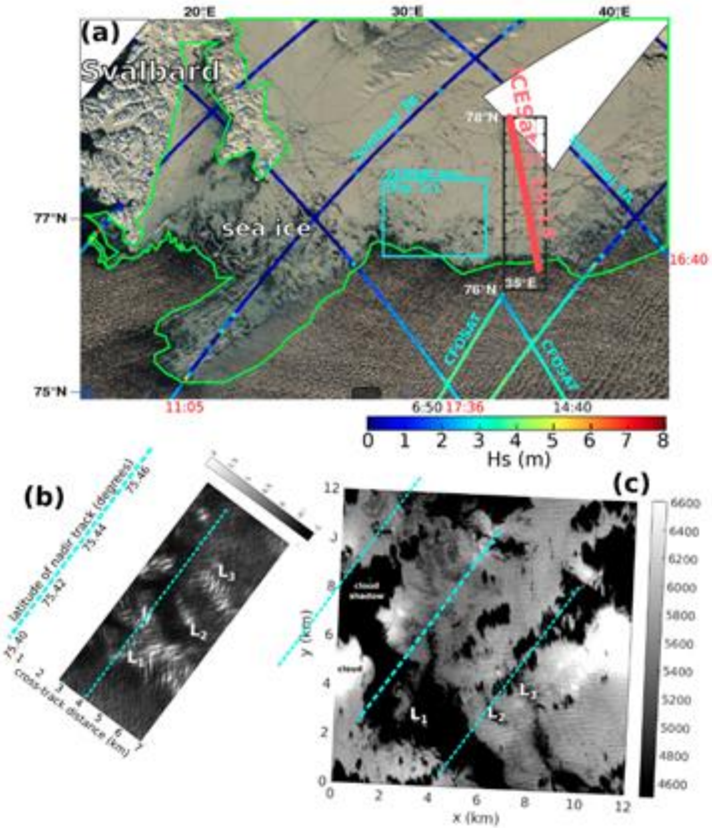

Wave amplitude attenuation in sea ice

- Example of unfiltered radar signature (blue line). Signal was obtained by cross-averaging of 200 m band aligned with wave propagation direction. Red line corresponds to detrended refined signal suitable for the envelope analysis. Black dashed line demonstrates estimated envelope.

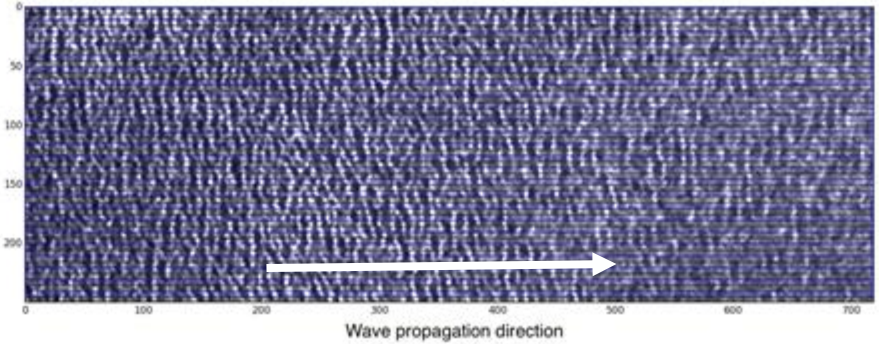

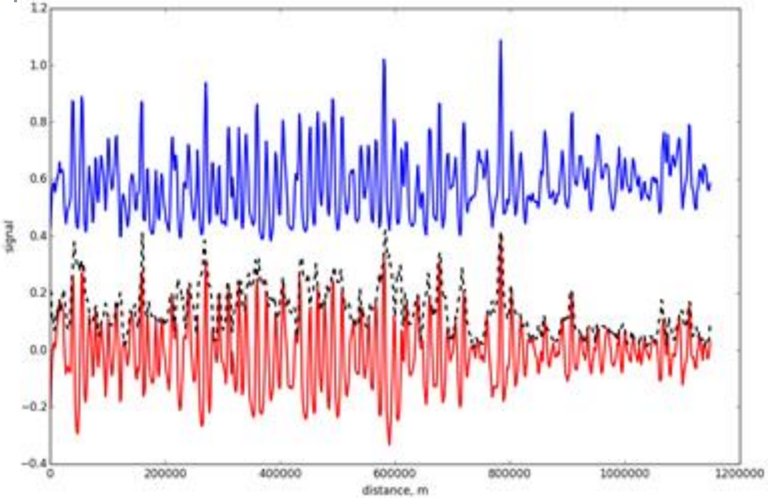

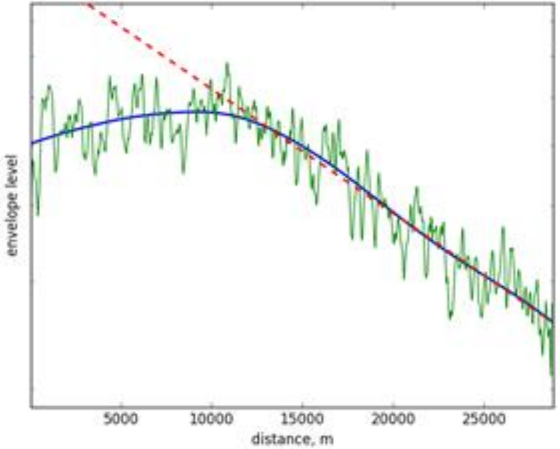

Polarimetric and multi-frequency observations

- Full-pol/compact-pol.
- RadarSat, GAOFEN, ROSE-L.
- Varying tilt and hydrodynamic sensitivity.
- Bragg to wave-breaking ratio.
- Effects of decorrelation (especially high sea states
- Affects modulations and cut-off.

- L-band and C-band crossovers.
- Sensitive to slightly different parts of the spectrum
- Different decorrelation.

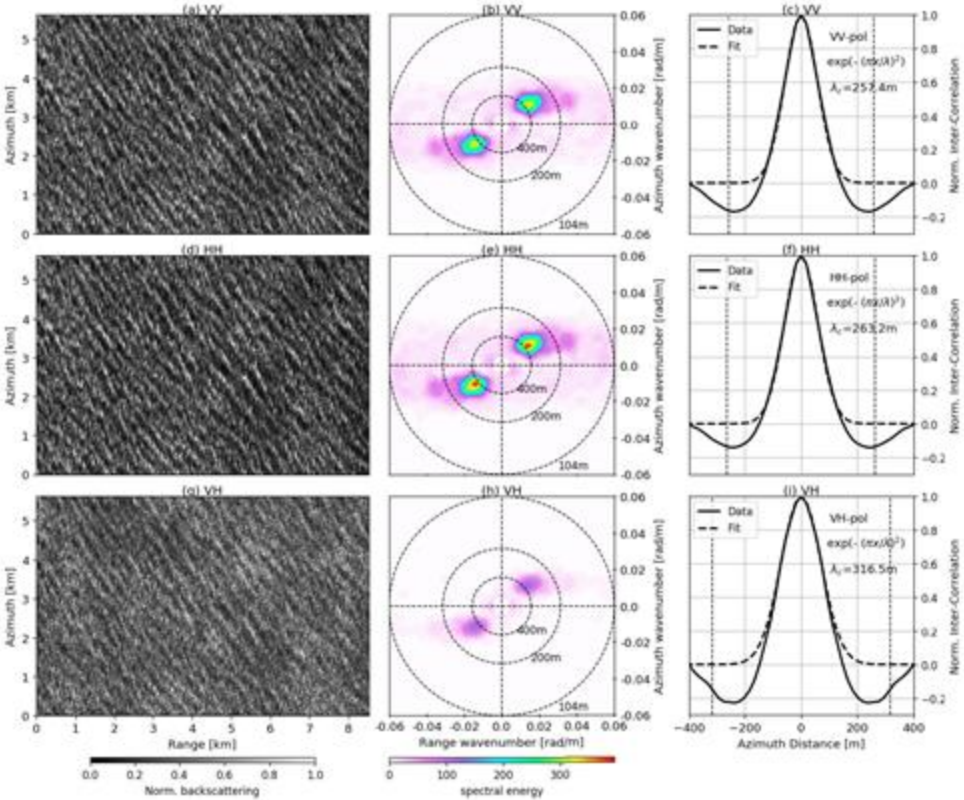

Figure from Li et al. (2019)

Wave-field continuity

- For image or wide swath mode, we can use continuity to remove outliers/ambiguities in neighboring swell direction. In deep oceand and small surface current, storm source refocussing is also used to ensure continuity.

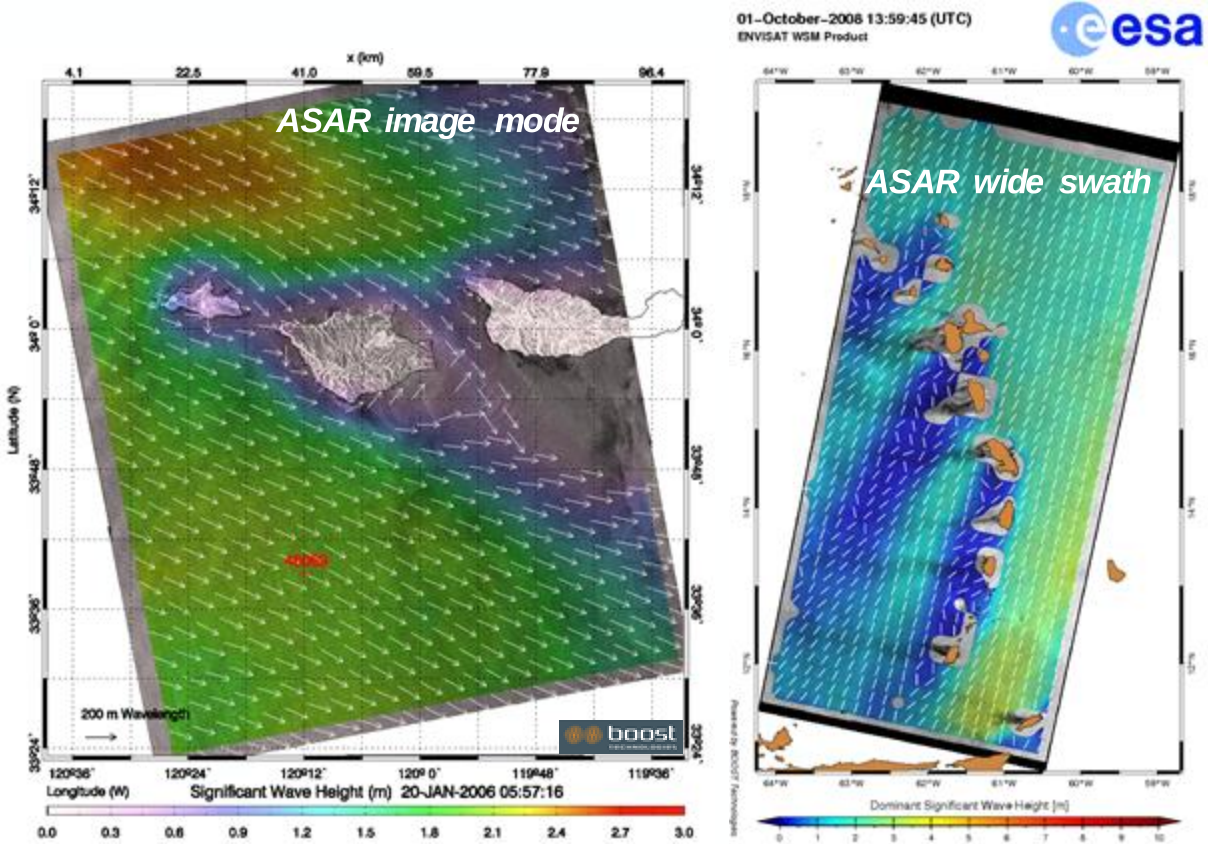

Wave amplitude demodulation (groups)

1. Spectral analysis.
2. wave systems decomposition.
3. Amplitude demodulation.
4. 2D Correlation length estimation.
5. Comparison between mean wave group direction and peak wave modulation direction.

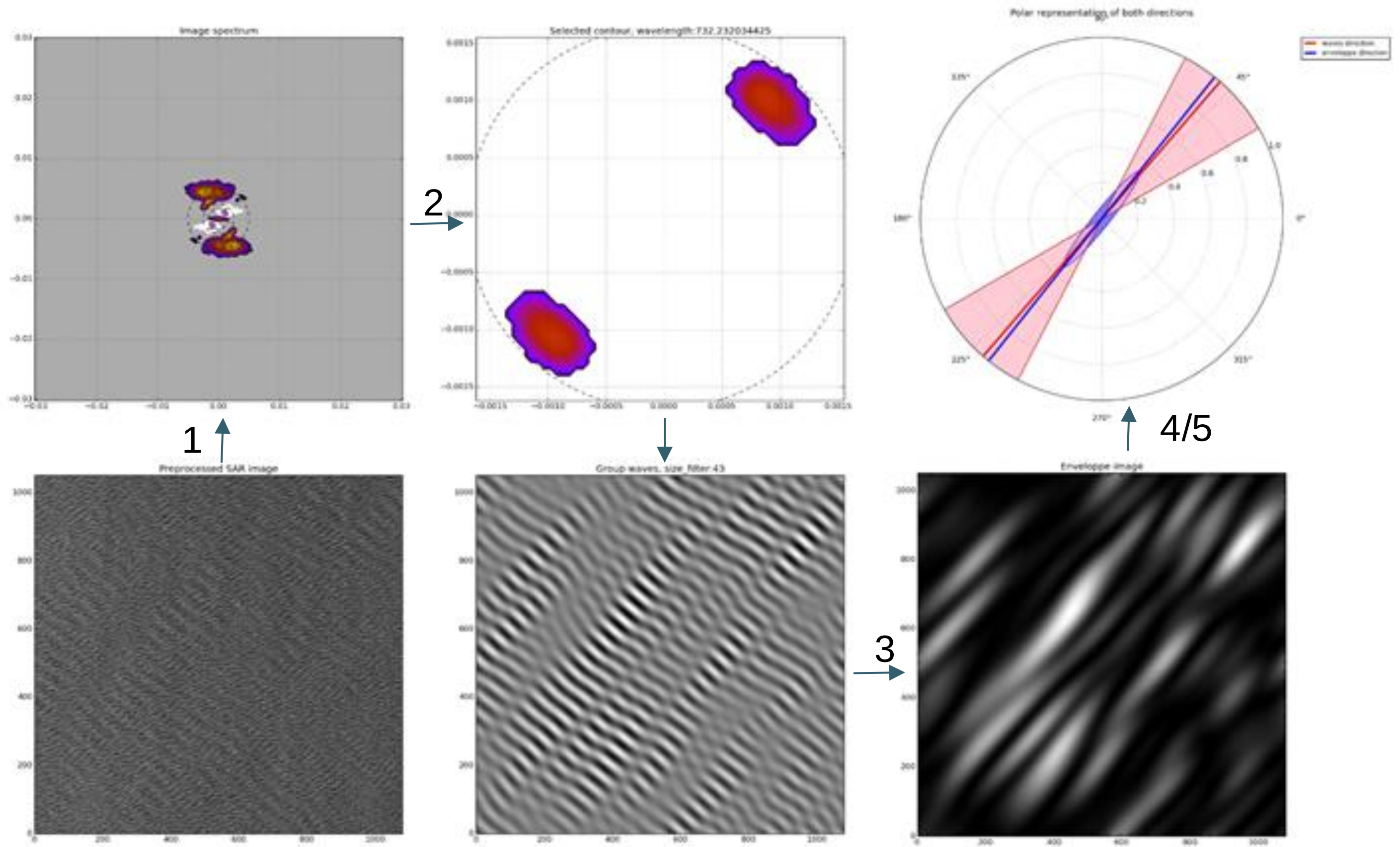

Wave amplitude demodulation (groups)

- 170m short swell not too much affected by azimuth cutoff.
- Mean group direction and peak direction in reasonable agreement.

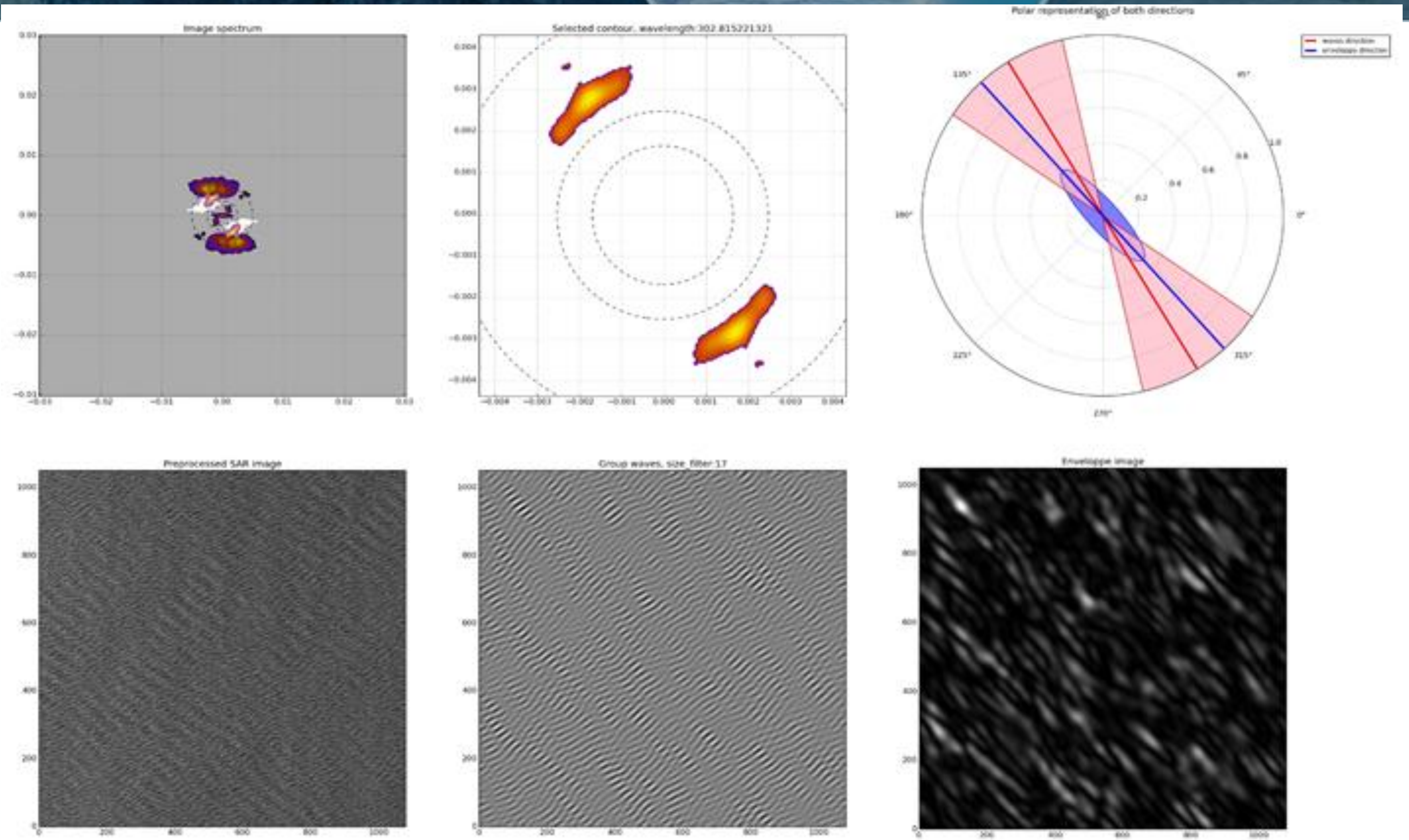

Wave amplitude demodulation (groups)

- 100m waves strongly affected by azimuth cutoff.
- Mean group direction and peak direction is not aligned anymore.

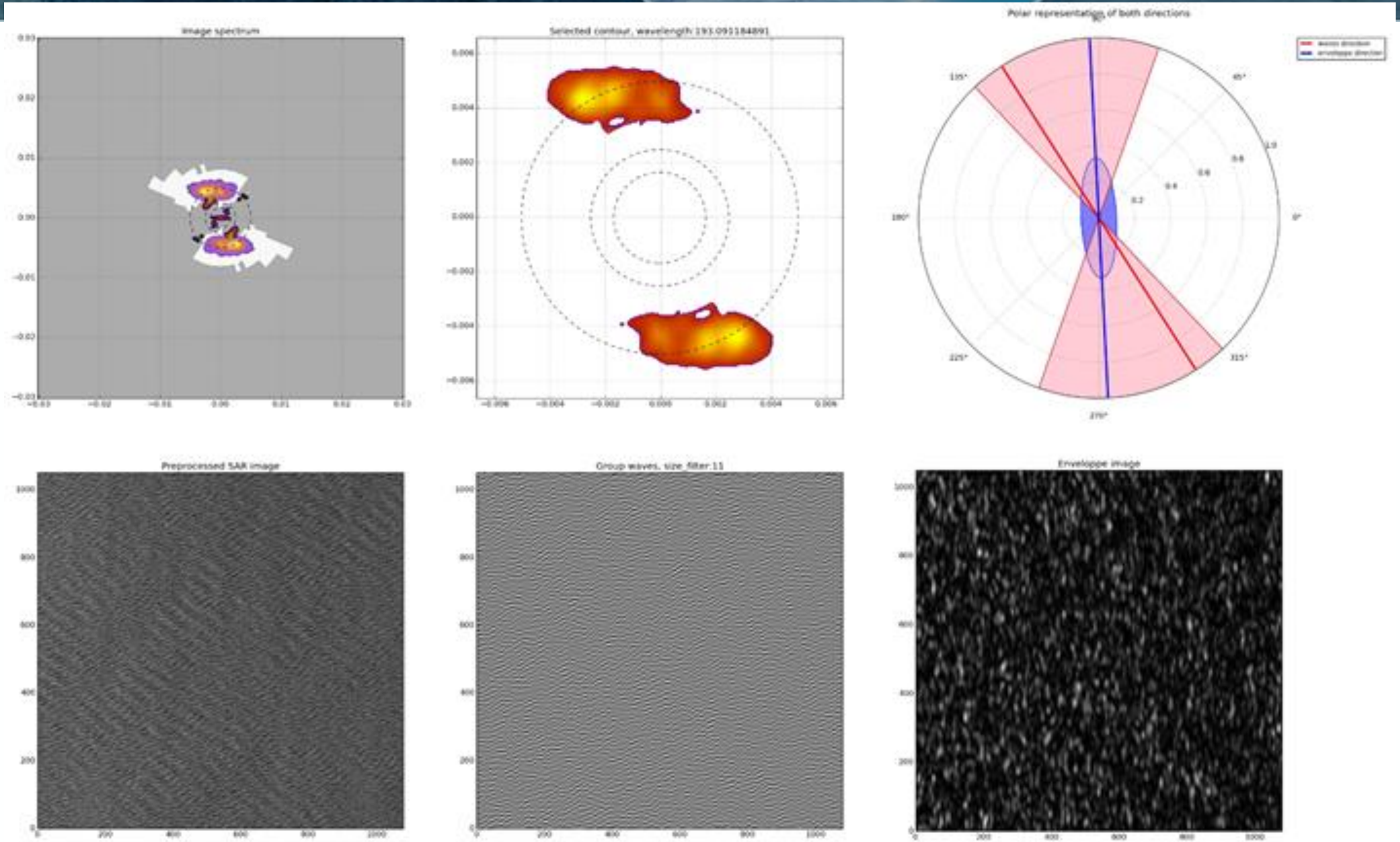

Multi-sensor synergies

- Sentinel-2 and wave drifters as ‘truth’.
- Spectra from SAR, altimetry and CFOSat.
- Wind(-wave) direction from scatterometry or models.

- Cross-calibration of ocean wave-spectra.
- More geometrical constraints.
- Sensitive to different parts of the wave spectrum.
- Integral multi-sensor approaches considering all scales.

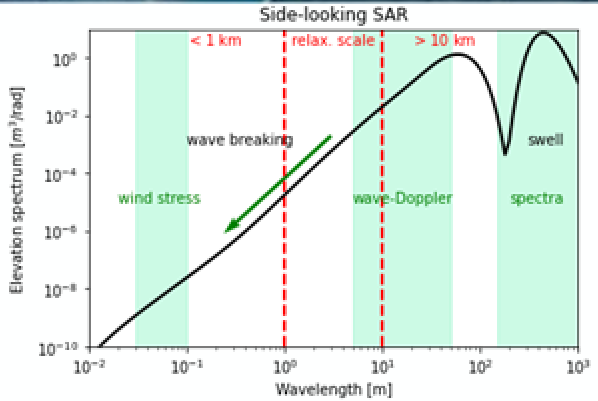

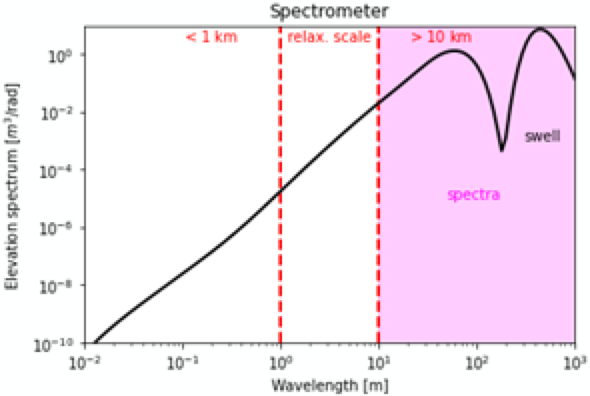

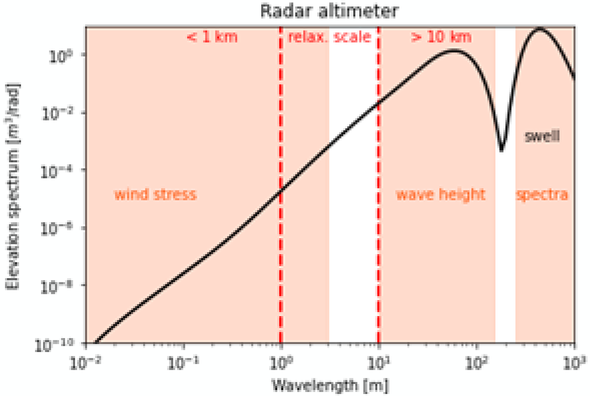

For visibility overlap is omitted.

Sentinel-2 sunglitter

- Satellite sun-glitter contains directional surface roughness information.
- Modulations of sun-glitter caused by long ocean waves.
- Requires favorable aligned of waves, sun and observing platform.

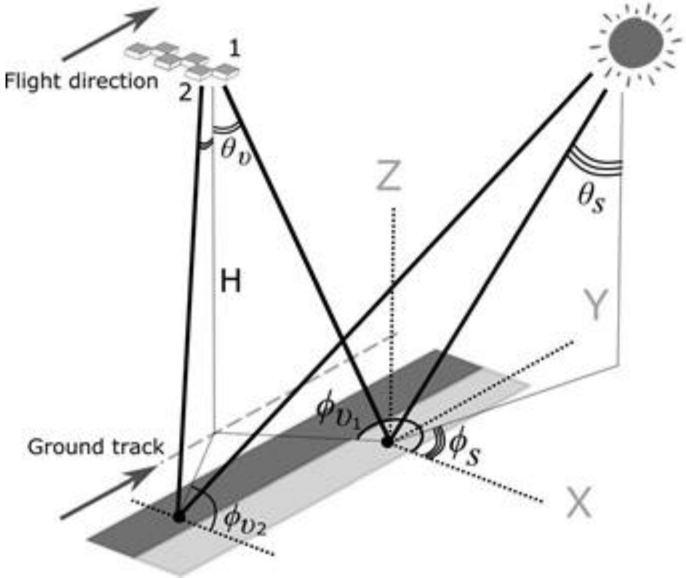

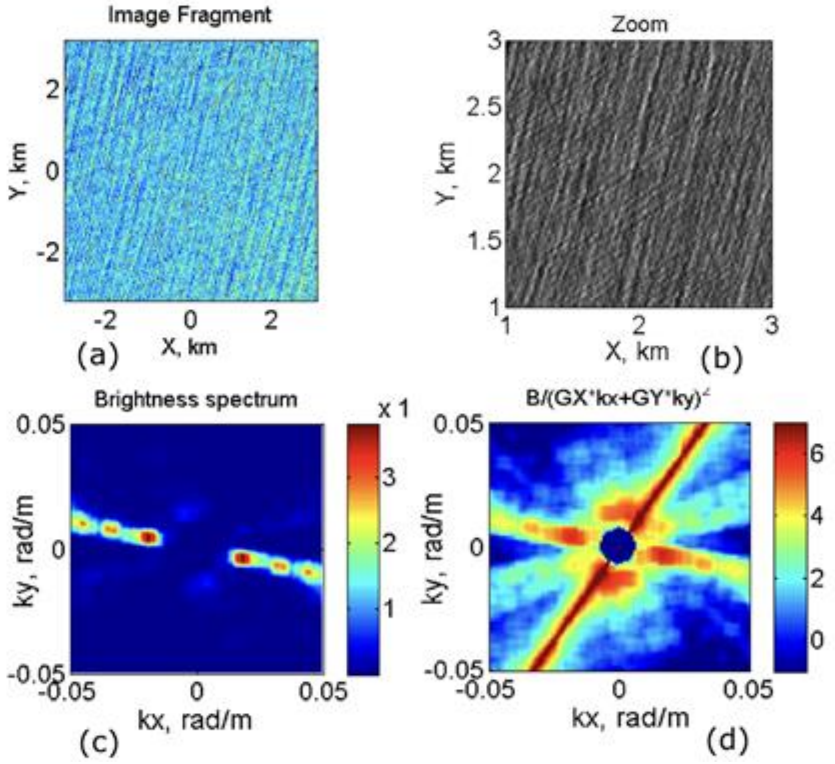

Figures from Kudryavtev et al. (2017)

Sentinel-2-derived wave spectra

- Multispectral images are collected one at a time.
- Time difference can be exploited to estimate the phase velocity.
- Cross-spectrum between B04 and B08 channels pick out “true” direction of wave components for descending (respectively ascending) satellite acquisitions.

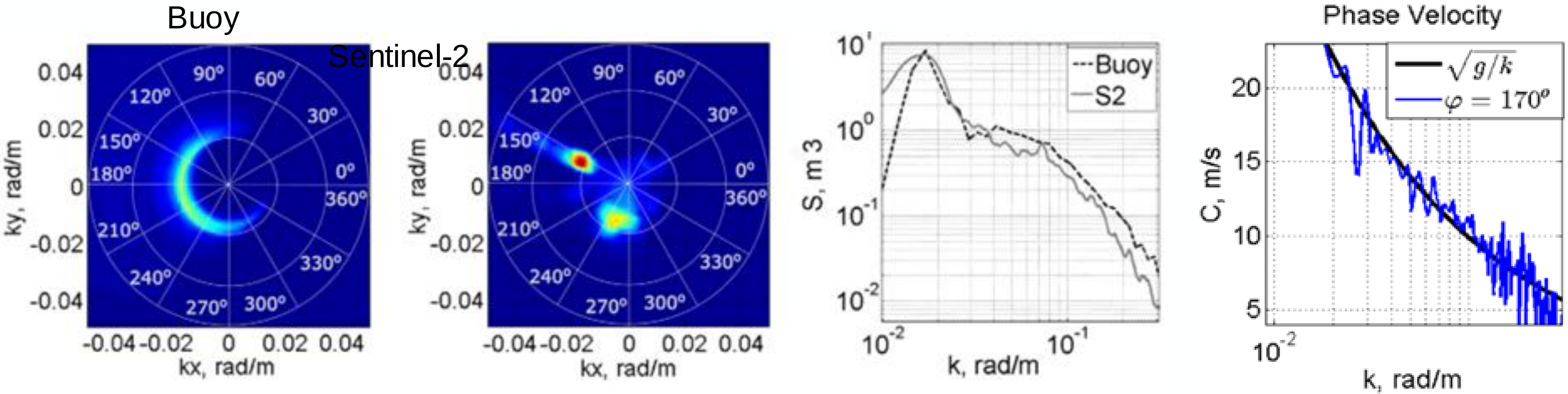

Figures from Kudryavtev et al. (2017)

SAR altimetry spectra

- Intensity modulation resulting from swell waves are visible in waveform tails.
- By normalization and reprojection on the ground it is possible to compute SAR spectra.
- Dominant mechanisms are velocity and range bunching.
- Only possible to retrieve swell in low to moderate sea states (SWH < 6 m).
- ‘Cut-off’ estimation (velocity variance) and swell retrieval might become essential to constrain the sea-state bias.

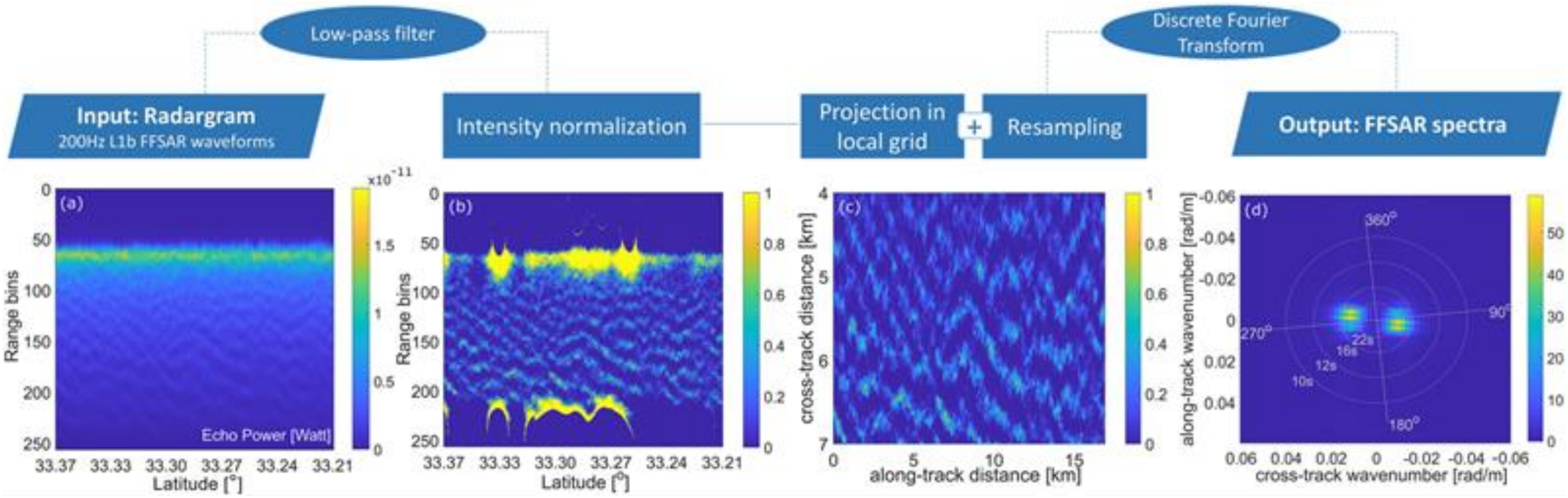

Figure from Altiparmaki et al. (2022)

SAR altimetry spectra

Rania Altiparmaki, Claire Maraldi, Samira Amraoui

PROJECTED/NORMALIZED RADAGRAM

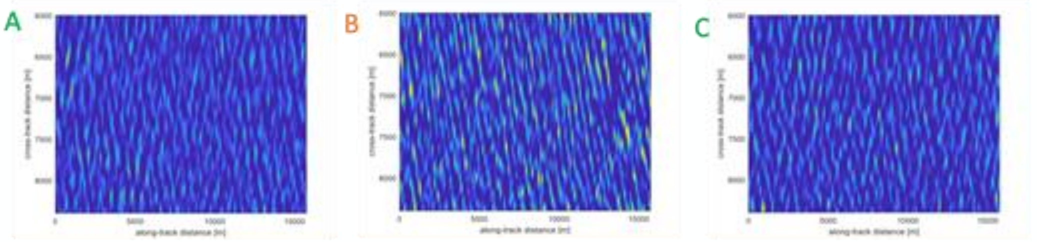

SAR SPECTRA

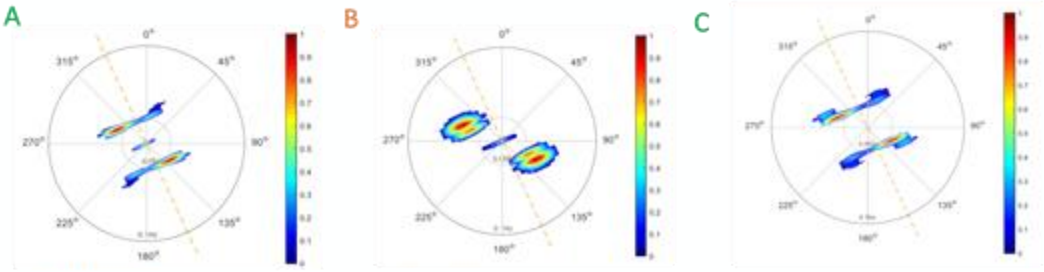

A: Tp =17.0 sec
Dp = 293 deg

B: Tp =15.1 sec
Dp = 293 deg

C: Tp =17.6 sec
Dp = 290 deg

ERA5 SWELL SPECTRUM

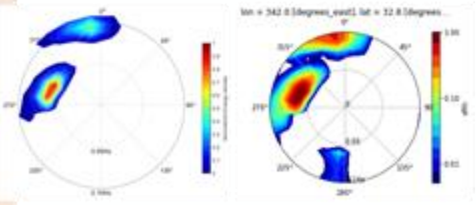

Tp = 15.8 sec
Dp = 292.5 deg

SAR altimetry cross-spectral analysis

- Zero-Doppler nadir-altimetry spectra have four ambiguities (both sides of track).
- Long overpass time O(2 s) allows for multiple sublooks and the generation of a cross-spectral stack.
- Modulations depend on geometry → rotation of cut-off, change of phase and sensitivity changes.

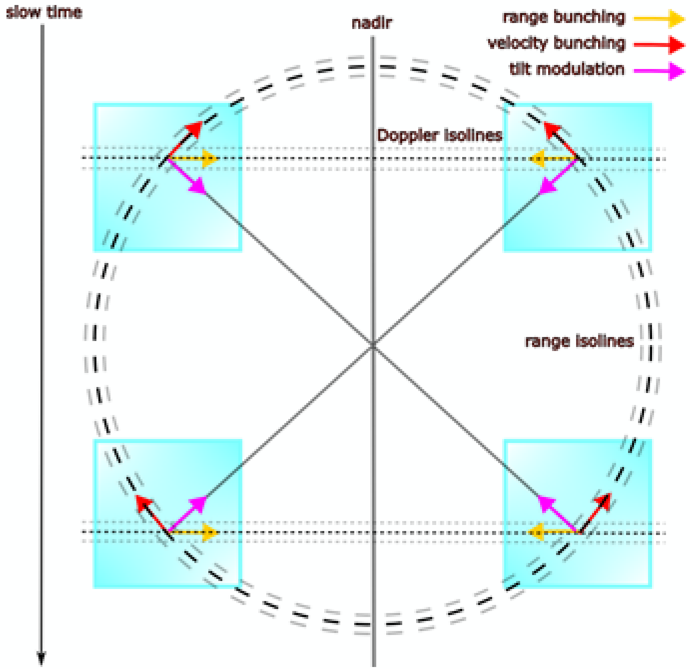

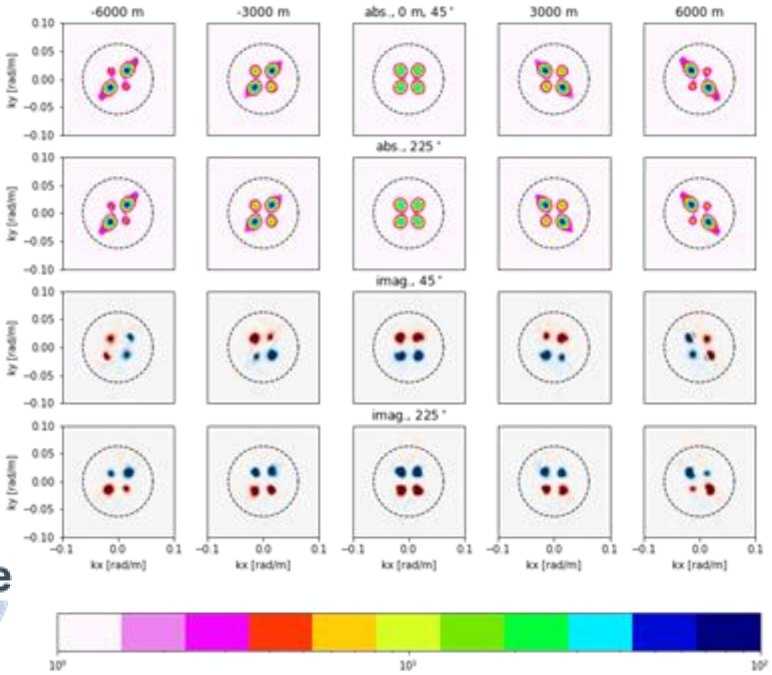

sarwave

Multi-scale Integrated Retrieval for Oceans (MIRO)

- High-resolution retrievals require multi-scale approaches and scene classification.
- NRCS, Doppler and SAR spectra originate from the same surface.
- NRCS, Doppler and SAR are originate from different wavelengths (and relaxation scales).
- Extend the deep-learning approaches.
- Adjoint wave modelling.
- Causal (iterative) filtering approaches.

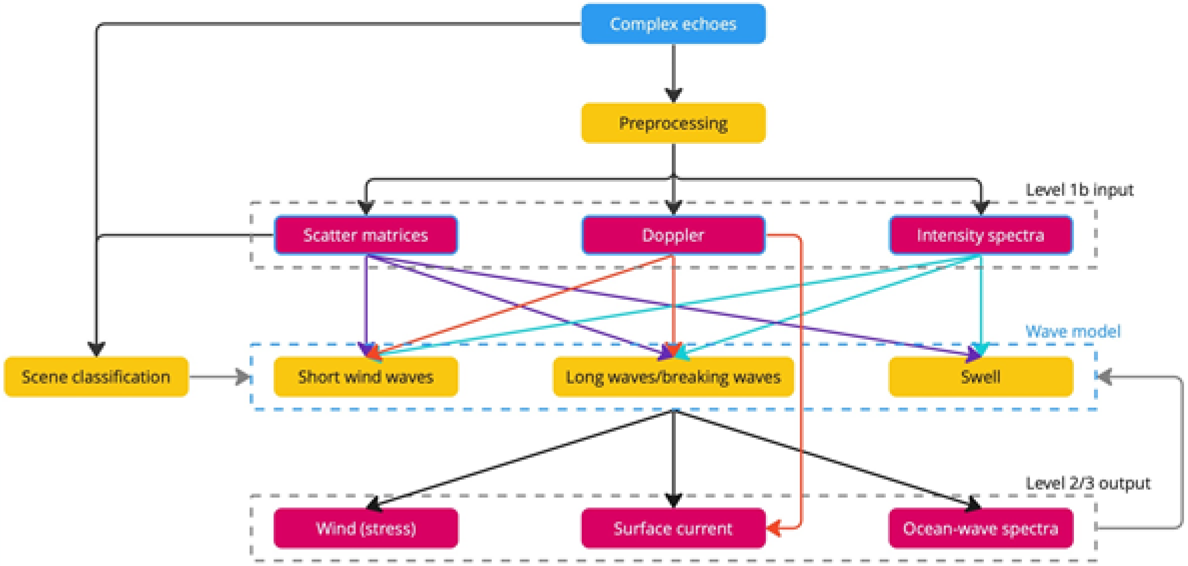

Toward an integrated approach for sea state retrieval

New opportunities and strategies for sea state parameter retrieval from RAW and complex (SLC) SAR acquisitions :

- Combination into a joint algorithm of Doppler, NRCS and x-spectra (MACS, CWAVE,...) quantities to retrieve wind/waves/current.
- Exploitation of wide-swath capabilities :
  - Take benefit of the expected spatial and temporal coherence of wind and waves fields on large scale.
  - Exploitation of the variability of the imaging mechanisms within the swath.
- Texture analysis (classification, wind properties, stability parameter, …).
- Sea state-driven SAR compression (L0 -> L1).

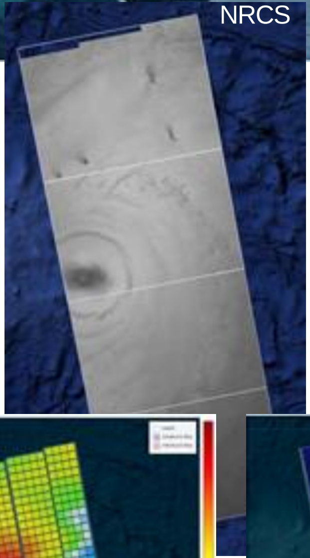

Cross spectra

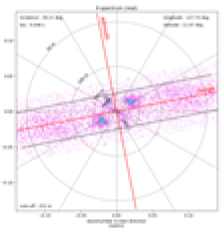

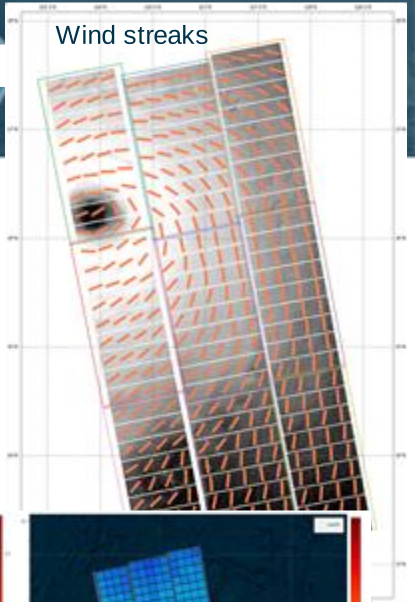

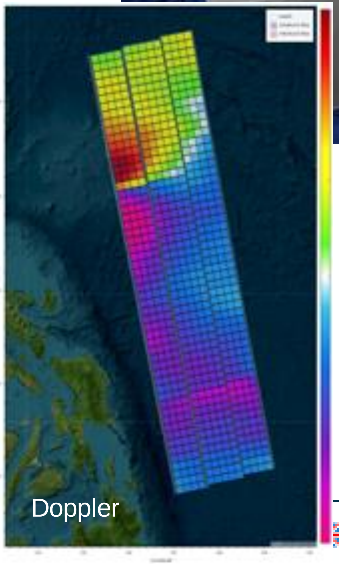

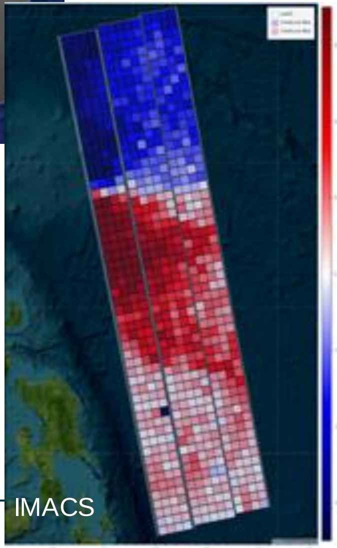

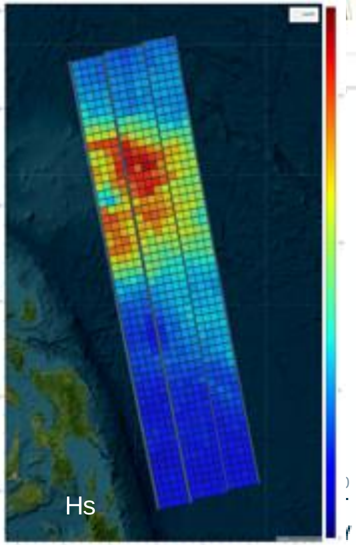

sarwave

Approved and proposed missions

- Bistatic SAR systems (**Harmony**)
- High-resolution multibeam SAR ATI (**SEASTAR**).
- Swath altimeters (**Sentinel-3 Next Generation**).
- Distributed systems (**SWARMSAR**).
- Dual-frequency altimeters (CRISTAL).
- L-band SAR systems (ROSE-L).
- Dual-frequency SAR systems (NISAR).
- Pencil-beam Doppler scatterometry.

Harmony

- Three lines-of-sight.
- Range and Doppler not perpendicular.
- Rotated sensitivity.
- Enhanced spectral coverage.

$$T_y = -\frac{R_t\omega}{2U_t}\left(\frac{k_x}{|k|}2\sin\theta_t + i2\cos\theta_t\right) = -\frac{R_t\omega}{U_t}\left(\frac{k_x}{|k|}\sin\theta_t + i\cos\theta_t\right)$$

$$T_x = \frac{-\omega\left(\frac{k_x}{|k|}(\sin\theta_t + \sin\theta_r\cos\alpha) - \frac{k_y}{|k|}\sin\theta_r\sin\alpha + i(\cos\theta_t + \cos\theta_r)\right)}{\left(U_t\cdot\frac{\delta\hat{r}_t}{\delta x} + U_r\cdot\frac{\delta\hat{r}_r}{\delta x}\right) + \left(U_t\cdot\frac{\delta\hat{r}_t}{\delta y} + U_r\cdot\frac{\delta\hat{r}_r}{\delta y}\right)\frac{\delta y}{\delta x}}$$

$$T_y = \frac{-\omega\left(\frac{k_x}{|k|}(\sin\theta_t + \sin\theta_r\cos\alpha) - \frac{k_y}{|k|}\sin\theta_r\sin\alpha + i(\cos\theta_t + \cos\theta_r)\right)}{\left(U_t\cdot\frac{\delta\hat{r}_t}{\delta x} + U_r\cdot\frac{\delta\hat{r}_r}{\delta x}\right)\frac{\delta x}{\delta y} + \left(U_t\cdot\frac{\delta\hat{r}_t}{\delta y} + U_r\cdot\frac{\delta\hat{r}_r}{\delta y}\right)}$$

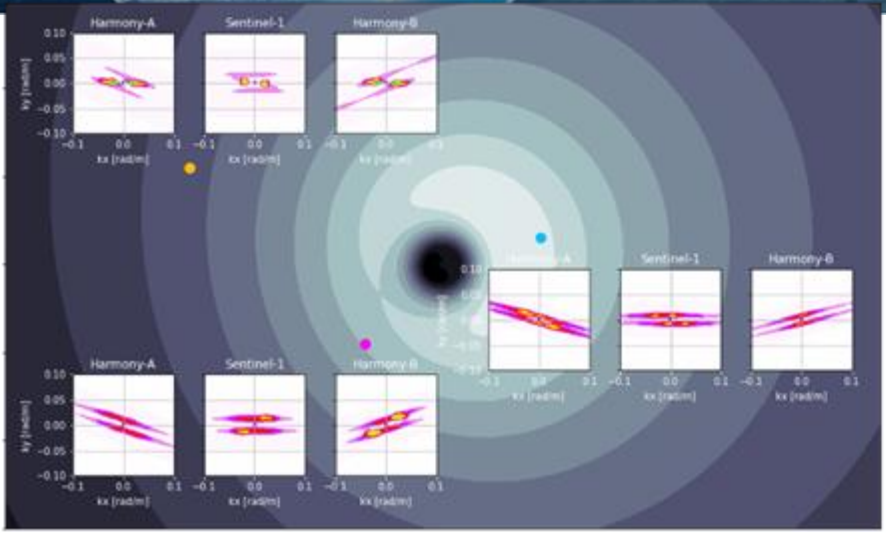

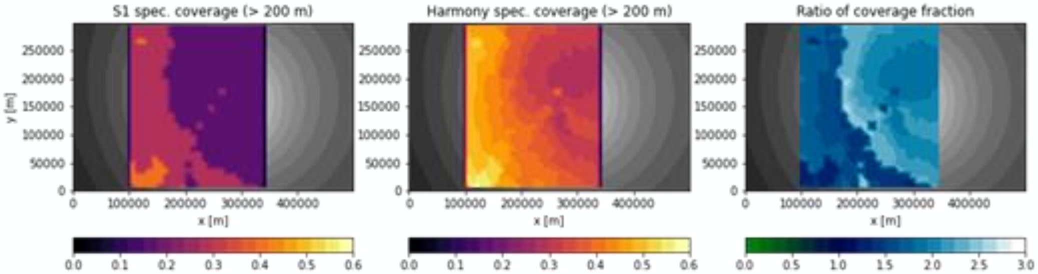

- Directional (i)MACS, cut-off and RAR.
- Polarimetric (i)MACS, cut-off and RAR.
- Additional constraints on the wind-wave system.

SEASTAR

- Better line-of-sight diversity than Harmony.
- Lower range resolution.
- Quad-pol transmission?

$$T_y = -\frac{R_t\omega}{2U_t}\left(\frac{k_x}{|k|}2\sin\theta_t + i2\cos\theta_t\right) = -\frac{R_t\omega}{U_t}\left(\frac{k_x}{|k|}\sin\theta_t + i\cos\theta_t\right)$$

$$T_x = \frac{-\omega\left(\frac{k_x}{|k|}\sin\theta\cos\alpha - \frac{k_y}{|k|}\sin\theta\sin\alpha + i\cos\theta\right)}{\left(\boldsymbol{U}\cdot\frac{\delta\hat{r}}{\delta x}\right) + \left(\boldsymbol{U}\cdot\frac{\delta\hat{r}}{\delta y}\right)\frac{\delta y}{\delta x}}$$

$$T_y = \frac{-\omega\left(\frac{k_x}{|k|}\sin\theta\cos\alpha - \frac{k_y}{|k|}\sin\theta\sin\alpha + i\cos\theta\right)}{\left(\boldsymbol{U}\cdot\frac{\delta\hat{r}}{\delta x}\right)\frac{\delta x}{\delta y} + \left(\boldsymbol{U}\cdot\frac{\delta\hat{r}}{\delta y}\right)}$$

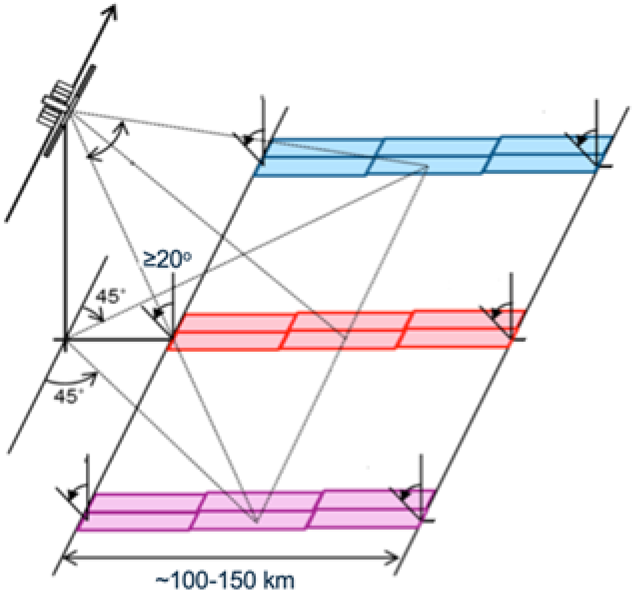

Gommenginger et al. 2019

Sentinel-3 Next Generation Topography

- Near-nadir incident angles.
- Velocity and range bunching dominant.
- Closed-form only applicable in low sea states.
  - Non-linear range bunching.
  - Supercritical waves.

$$\lambda_c \propto \pi\sqrt{\rho_{yy}(0,0)} = \pi\frac{H}{V}\sqrt{\sigma_v^2}$$

$$\lambda_{ct} \propto \pi\sqrt{\rho_{xx}(0,0)} = \pi\sqrt{\frac{\sigma_e^2}{\tan^2(\theta)}} = \pi\frac{\text{SWH}}{4\tan(\theta)}$$

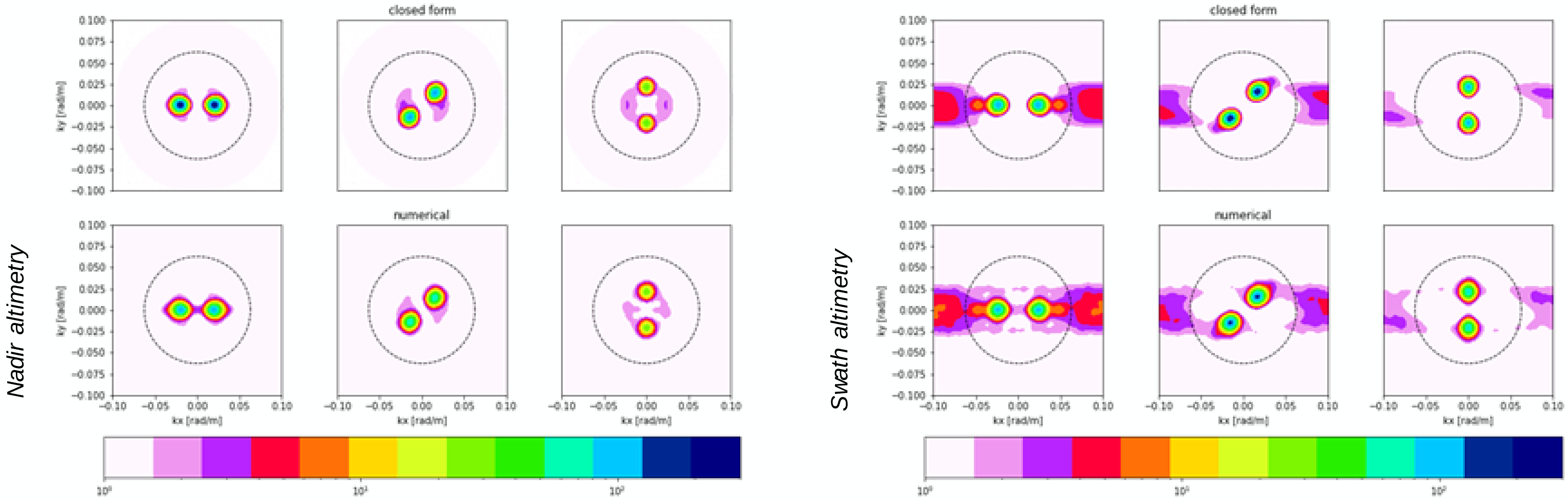

SWARMSAR

- SwarmSAR is a MIMO like configuration
- All nodes illuminate the same area of interest
- Each node has a basic imaging capabilities
- Resolution capabilities increase when nodes work together.

Parameters	Value
Satellites height	693 km
Satellite Separation	100 m
Satellites velocity	7000 km/h
Operating frequency	2.9 GHz (S-band)
Wind speed	10 m/s
Correlation Time	30 ms
No. of Sensors	5

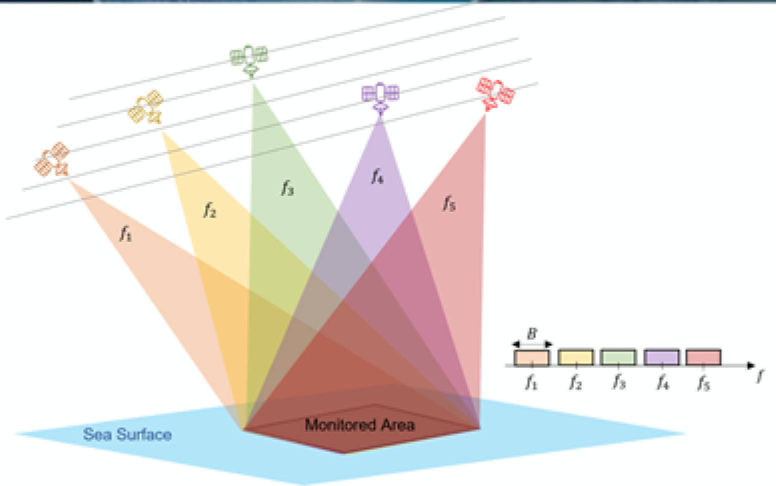

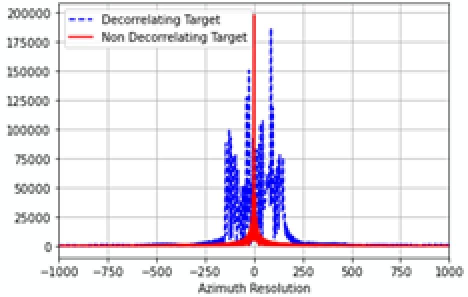

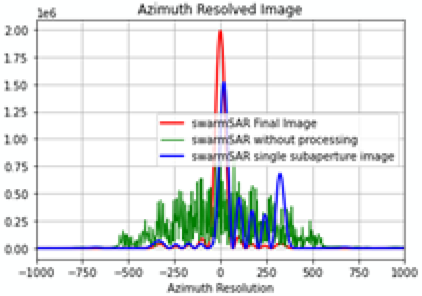

Summary and conclusions

- SAR retrieval algorithms:
  - Limited improvements in closed-form retrievals (~2003-2020).
  - Emergence of (parametrized) neural-network approaches (~2005-2020).

- Current work (~2020-2023):
  - Improvements in the closed-form model and inversion.
  - Exploitation of continuity in wave fields (Fireworks).
  - Deep-learning retrievals.
  - Assimilation of wave data into models.
  - Multi-sensor approaches.
  - Satellite radar altimetry as a new source for wave-spectrum estimation.
  - Retrieval algorithms for proposed and approved missions.
  - SARWAVE: https://www.sarwave.org/

Recommendations

- Learn RAR MTF from IW data exploiting all possible polarisations.
- Use of rapidly growing wave drifter network oven open ocean and sea ice for learning and validation.
- Use wave retrieval in sea ice for MIZ monitoring.
- Explore wave retrieval methods before azimuth SAR focusing to avoid image distortion.
- Make an open source wave-spectra-retrieval algorithm library, out of existing up to date knowledge.

Recommendations

- Multi-sensor synergies:
  - Different sensors are sensitive to different parts of the wave spectrum.
  - Better constraints at cross-overs.
  - Cross-calibration.

- Multiscale Integrated Retrievals for the Ocean (MIRO) algorithms:
  - Wind stress, wave-Doppler, currents and long-wave spectra should not be estimated separately.
  - Multiscale retrievals based on deep-learning approaches.
  - Causal filtering and/or external models should be computed.
  - Continuity constraints on the wave field (Fireworks/IW mode).
  - Possibly iterative methods.

- Future missions:
  - Benefit from MIRO algorithms.
  - Line-of-sight diversity.
  - Synoptic, high-resolution view of the air-sea interface.